A post-Newtonian approach to neutron star oscillations

Shanshan Yin* and Nils Andersson[†]

Mathematical Sciences and STAG Research Centre,
University of Southampton, Southampton SO17 1BJ, United Kingdom

Fabian Gittins[‡]

Institute for Gravitational and Subatomic Physics (GRASP), Utrecht University, Princetonplein 1, 3584 CC Utrecht, Netherlands and Nikhef, Science Park 105, 1098 XG Amsterdam, Netherlands

Next-generation gravitational-wave detectors are expected to constrain the properties of extreme density matter via observations of static and dynamical tides in binary neutron star inspirals. The required modelling is straightforward in Newtonian gravity—where the tide can be represented in terms of a sum involving the star's oscillation modes—but not yet fully developed in general relativity—where the mode-sum approach is problematic. As a step towards more realistic models, we are motivated to explore the post-Newtonian (pN) approach to the problem (noting that the modes should still provide an adequate basis for a tidal expansion up to 2pN order). Specifically, in this paper we develop the pN framework for neutron star oscillations and explore to what extent the results remain robust for stars in the strong-field regime. Our numerical results show that the model is accurate for low-mass stars ($\lesssim 0.8 M_{\odot}$), but becomes problematic for more massive stars. However, we demonstrate that the main issues can be resolved (at the cost of abandoning the consistency of the pN expansion) allowing us to extend the calculation into the neutron star regime. For canonical neutron stars ($\approx 1.4 M_{\odot}$) our adjusted formulation provides the fundamental mode of the star with an accuracy comparable to that of the relativistic Cowling approximation. For lower mass stars our approach performs is significantly more accurate, suggesting that a pN formulation of the tidal problem is, indeed, warranted.

I. INTRODUCTION

The properties of cold dense matter above the nuclear saturation density remain relatively poorly constrained by experiment and astrophysical observations (see [1] for a recent review). As a result, the precise nature of the matter deep inside neutron stars is still uncertain. This uncertainty is typically encoded in the equilibrium equation of state for matter, a relation providing the thermodynamic pressure as a function of energy density (temperature, matter composition, etcetera). This microscopic relation is required to determine the macroscopic properties—essentially, the mass-radius relation—of neutron stars (via the Tolman-Oppenheimer-Volkoff equations) which can then be tested against observational data. The current state-of-the-art for tests based on electromagnetic observations draws on data from NASA's Neutron Star Interior Composition Explorer (NICER) mission [2–5].

Gravitational-wave observations of compact binaries involving at least one neutron star open another promising avenue for exploration. Specifically, observational constraints on the tidal deformability [6, 7]—encoding the response of a neutron star to the tide induced by a binary companion—provide information on the neutron star radius. The tightest such constraints to date were obtained for GW170817 [8, 9], the first observed binary neutron star system, with weaker constraints inferred from the subsequent GW190425 event [10]. The current error bars on the neutron star radius inferred from gravitational-wave data are similar to those gleaned from NICER.

Future gravitational-wave observations, with more sensitive instruments like the Einstein Telescope [11] and Cosmic Explorer [12], are expected to lead to significantly tighter constraints (see, for instance, the discussion in [13]). In addition to probing the mass-radius relation, we expect to gain insight into the composition and state of matter in the neutron star core. This involves important issues like the presence of hyperons and/or deconfined quarks, various macroscopic superfluid/superconducting components and so on. In order to explore these aspects, we need to look behind the static tidal deformability and consider the impact of dynamical tides [14–17]. During a binary inspiral, the tidal field of the companion induces a time-varying mass-quadrupole moment, deforming the star, enhancing the gravitational-wave emission and accelerating the coalescence. As the orbital separation approaches the size of the bodies, the stars' internal structure become important. In particular, the tidal force excites individual stellar

^{*} shanshan.yin@soton.ac.uk

[†] n.a.andersson@soton.ac.uk

[‡] f.w.r.gittins@uu.nl; Author to whom any correspondence should be addressed

oscillation modes—as they become resonant with the tidal driving [18, 19]—leading to additional transfer of orbital energy into the stellar fluid, potentially having an observable impact on the orbital evolution. This is the dynamical tide

The dynamical tide manifests in a number of ways. The dominant contribution is associated with the star's fundamental f-mode [14–16]. This mode may not reach actual resonance before merger, but its presence nevertheless leads to a notable enhancement of the tidal response. Models that do not include this enhancement introduce an unnecessary systematic bias in the extracted neutron star parameters (and hence the equation of state constraints) [17]. At a more subtle level, a number of low-frequency modes may be dynamically excited as the system sweeps through the sensitivity band of a detector. The most likely such resonances are associated with gravity modes linked to the matter composition [20] and possible interface modes associated with internal phase transitions (e.g. the crust-core transition [21–23] or a first order phase transition to an exotic matter phase at higher density) [24, 25]. The problem is even richer for rotating stars. Not only does stellar rotation shift the mode resonances (e.g. making the f-mode resonance more likely before merger) [26–28], it also brings new modes into existence. The most promising of these so-called inertial modes is thought to be the r-mode [29, 30], which couples to the tide gravitomagnetically [31, 32].

The possibility that dynamical tide features may be within reach of observations motivates a detailed analysis for next-generation detectors, like the Einstein Telescope and Cosmic Explorer. In parallel with the design of these instruments, we need to improve our theoretical models. This involves accounting for all relevant aspects (or, at least, as many as we can manage...) of neutron star physics. A key part of this effort involves improving on the Newtonian mode-sum approach, which is commonly used to model dynamical tides [18, 19]. The idea behind this approach is simple. If the oscillation modes of a star form a complete set then they can be used as a basis to represent the tidal deformation as a sum of modes. In Newtonian gravity this is the case [33, 34]. However, it is not expected to remain true in general relativity [35–40]. The main difficulty in general relativity is that the modes are not going to be complete (due to the existence of late-time power-law tails associated with wave scattering by the curved spacetime) and the gravitational-wave damping also makes the problem non-Hermitian [41]. This presents a technical challenge that we need to overcome if we want to use realistic matter physics in our models for the dynamical tide, the study on which adopting different approaches can be found: the relativistic tidal response in the low frequency regime [42, 43], the description of dynamical tides through mode decomposition and matching with the post-Newtonian solutions [44], or using the effective one body model [15]; the calculations of the tidal resonance using the wave scattering method [45] etc.

A possibly way to progress the discussion would be to explore the problem within post-Newtonian theory. While post-Newtonian (pN in the following) models are not expected to be very accurate for relativistic stars one would expect them to be decidedly better than Newtonian ones. In particular, one may build post-Newtonian models for realistic equations of state [46]. In addition, one should be able to develop a post-Newtonian mode-sum strategy for tides as the set of stellar oscillation modes is believed to remain complete up to 2pN order (see the arguments in [47]). It would thus seem, at least conceptually, relevant to pursue this strategy. Ultimately, the effort may only represent a small step towards a more accurate description of dynamical neutron-star tides but we still hope to learn useful lessons from the analysis. As a necessary step in this direction, we calculate neutron star oscillation modes in post-Newtonian theory in this paper.

The paper is organised as follows. To begin with, in section II we build neutron stars in pN theory. We then formulate the pN oscillation problem in section III and discuss our numerical results in section IV. Finally, we conclude in section V. Unless otherwise indicated we use geometric units in which c = G = 1.

II. BUILDING POST-NEWTONIAN NEUTRON STARS

The definitive treatise of the modern approach to the post-Newtonian method was provided by Poisson and Will about a decade ago [48]. They describe the foundations of the approach and its links to both Newtonian gravity and Einstein's theory. This exhaustive text provides a natural starting point for a range of relevant applications. In particular, the problem of tides raised in compact binaries is laid out in detail. Having said that, there is still room for the development of applications connecting with other aspects of physics. For the tidal problem, a natural question relates to modern matter equations of state obtained from nuclear physics arguments. This is the issue that motivates the effort we present here. We want to explore to what extent we can make progress on modelling dynamical neutron star tides within the pN framework. The reason for exploring this question is not an expectation that a pN model would be exceptionally precise. Not at all! We are quite realistic in this respect and already know from [46] that the stellar models built within the pN framework will deviate significantly from their relativistic counterparts in the neutron star regime. However, we also note that the problem of fully relativistic dynamical tides involves a number technical challenges (see [42] for a recent discussion). Intuitively, one might expect some of these issues to be absent

in (low-order) pN theory. For example, the formulation of a mode-sum for the tidal response—the go-to approach in Newtonian tidal theory that is not expected to be (at least not easily) extendable to general relativity—can be formulated in the pN framework [47]. Given this, it is interesting to pursue the problem and see how far we get.

An important feature of a pN model is that, by including matter terms of order $1/c^2$, we can account for the internal energy of matter and hence work with realistic neutron star equations of state [46]. There is, however (and famously!), no such thing as a free lunch. The main problem we face is hard wired into the pN strategy. Notably, in pN hydrodynamics [48] it is customary to carry out the calculation in such a way that equations are truncated at a specific order in a $1/c^2$ expansion, yet allowing some higher order terms to remain. As long as we operate in the strict weak-field regime, the presence of these higher order terms is irrelevant. They are all small. However, neutron stars have moderate to strong internal gravitational fields so the higher terms that are kept in the calculation will impact on the results. This is (obviously) not a nice feature. Having said that, the alternative—to carry out a strict order by order pN expansion (as in the calculations reported in [49])—is not an attractive proposition either (for reasons explained in [47]). At the end of the day, we need to work through the calculation if we want to assess the quality of the results. Building on the work in [46] on static post-Newtonian fluid configurations and our recent analysis of the Hermitian properties of pN fluid perturbations in [47] we set out to formulate and solve the problem of calculating oscillation modes in the pN framework. The calculation we carry out shares many aspects with the recent work in [50]. The one important distinction is that, while that work applies the method to white dwarfs (where the pN approach should be "safe"), our intention is to push the calculation into the strong-field regime relevant for neutron stars to find out if, when and how it breaks.

In order to solve the perturbation problem, we need to start from a suitable background configuration. Our previous work [46] provides useful models in this respect, but also raises the warning flag we have already alluded to. Because of the inclusion of higher order pN terms, there is a significant degree of freedom in building stellar models. The presence of higher order terms dictates (quite naturally) the density at which a given model "breaks down", but some formulations perform better than others. This introduces a certain element of "black magic" (not an uncommon feature in approximation theory) which we need to keep in mind in the following.

Having made these cautionary remarks, we consider two of the models formulated in [46]. Our first model, from now on referred to as PW, builds on the discussion in the monograph of Poisson and Will [48]. The second model, in the following referred to as AGYM, builds on work by Andersson et al [46] and involves a physically motivated reformulation that leads to more accurate neutron star models.

In order to explore the neutron star oscillation problem, we need to first construct suitable equilibrium background models. These background stars are spherically symmetric, static configurations involving a perfect fluid described by the (baryon) mass density ρ , the internal energy density per unit mass Π and the pressure p. The fluid's internal energy per unit mass Π is related to the total energy density ε through

$$\varepsilon = \rho c^2 + \rho \Pi \ . \tag{2.1}$$

In the PW model the gravitational potential, U, is sourced by the baryon mass, M_B , which satisfies

$$\frac{dM_B}{dr} = 4\pi \rho^* r^2 \,, \tag{2.2}$$

and which leads to

$$\frac{dU}{dr} = -\frac{GM_B}{r^2} \ . \tag{2.3}$$

The model involves a rescaled mass density ρ^* [48], defined by

$$\rho^* = \rho \left(1 + \frac{3U}{c^2} \right) . \tag{2.4}$$

It is also worth noting that—as is commonly the case in post-Newtonian models—the radial distance r is expressed in the isotropic coordinates [46]. At 1pN order we also need the mass \mathcal{N} , given by

$$\frac{d\mathcal{N}}{dr} = 4\pi \rho^* r^2 \left(\Pi - U + \frac{3p}{\rho^*} \right) . \tag{2.5}$$

With these definitions, the equation for hydrostatic equilibrium takes the form

$$\frac{dp}{dr} = -\frac{G\rho^*}{r^2} \left\{ M_B + \frac{1}{c^2} \left[\left(\Pi - 3U + \frac{p}{\rho^*} \right) M_B + \mathcal{N} \right] \right\} . \tag{2.6}$$

It is worth noting that that, as ρ^* is involved in the equations, the calculation is not consistently truncated at 1pN order. In fact, as written here, the right-hand side of (2.6) include 3pN terms. Formally, the presence of the higher order terms does not matter but they will impact on the numerical results in the strong-field regime.

To build a pN neutron star model, we pick an initial value for the potential, $U(r=0) = U_0$, at the centre, integrate the above equations to the point where the pressure vanishes p(R) = 0. This defines the stellar surface, r = R. Then we execute a root search to determine U_0 by matching the potential at the surface to the exterior in such a way that

$$U(R) = \frac{GM_B(R)}{R} \,. \tag{2.7}$$

In contrast, the AGYM model combines variables in such a way that the gravitational potential is sourced by the gravitational mass M (as would be the case in general relativity). To effect this, we introduce the gravitational mass

$$M = M_B + \frac{1}{c^2} \mathcal{N} , \qquad (2.8)$$

which satisfies

$$\frac{dM}{dr} = 4\pi \rho^* \left[1 + \frac{1}{c^2} \left(\Pi - U + \frac{3p}{\rho} \right) \right] r^2 . \tag{2.9}$$

and leads to the gravitational potential being determined by

$$\frac{dU}{dr} = -\frac{GM}{r^2} \,. \tag{2.10}$$

By discarding some (not all!) 2pN terms from (2.6), we can write the hydrostatic equilibrium equation in the alternative form

$$\frac{dp}{dr} = -\frac{G\rho^*}{r^2} \left[M + \frac{1}{c^2} \left(\Pi - 3U + \frac{p}{\rho^*} \right) M_B \right] \approx -\frac{GM\rho}{r^2} \left[1 + \frac{1}{c^2} \left(\Pi + \frac{p}{\rho} \right) \right] = -\frac{GM}{r^2 c^2} (p + \varepsilon) . \tag{2.11}$$

The presence of $p + \varepsilon$ is a key feature of the fully relativistic problem.

For the AGYM model the surface boundary condition changes to

$$U(R) = \frac{GM(R)}{R} \,. \tag{2.12}$$

If we want to compare to relativistic models obtained from the standard Tolman-Oppenheimer-Volkoff equations then the stellar radius R in isotropic coordinates can be easily transformed to Schwarzschild coordinates (R_S) through

$$R_S = R\left(1 + \frac{GM}{2Rc^2}\right)^2 \ . \tag{2.13}$$

The two formulations, PW and AGYM, notably differ only in terms that contribute beyond 1pN order. Nevertheless, we know from the discussion in [46] that they lead to rather different mass-radius relations for neutron star densities. These results were established for an equation of state based on nuclear physics arguments (specifically from the BSk family of models [51, 52]). However, as the present analysis is more at the level of a proof-of-principle and the numerical implementation of realistic matter models is somewhat more involved, we instead focus on a phenomenological polytropic matter model. That is, we use

$$p = K \rho^{\Gamma} \,, \tag{2.14}$$

where ρ is the rest mass density, K is a constant and $\Gamma = 1 + 1/n$ with n the polytropic index. Combined with the thermodynamical relation (A1) the internal energy Π then has the form

$$\Pi = \frac{K\rho^{\Gamma - 1}}{\Gamma - 1} \,. \tag{2.15}$$

The specific stellar models we consider follow from using $K = 185 \text{ km}^2$ and $\Gamma = 2$, which allows for the existence of a solution to the Tolman-Oppenheimer-Volkoff equations with the canonical neutron star mass of $1.4M_{\odot}$, see Figure 1. These parameters are, of course, still not particularly realistic because the maximum mass reached by the model is far too low. This lack of realism is not a major concern for us, though, because the results in Figure 1 also show that the pN configurations deviate from the relativistic results already at lower densities. Our main interest is in the phenomenology. We want to see if the "problematic" features of the background models are inherited by the perturbations and explore to what extent additional complications enter the oscillation problem.

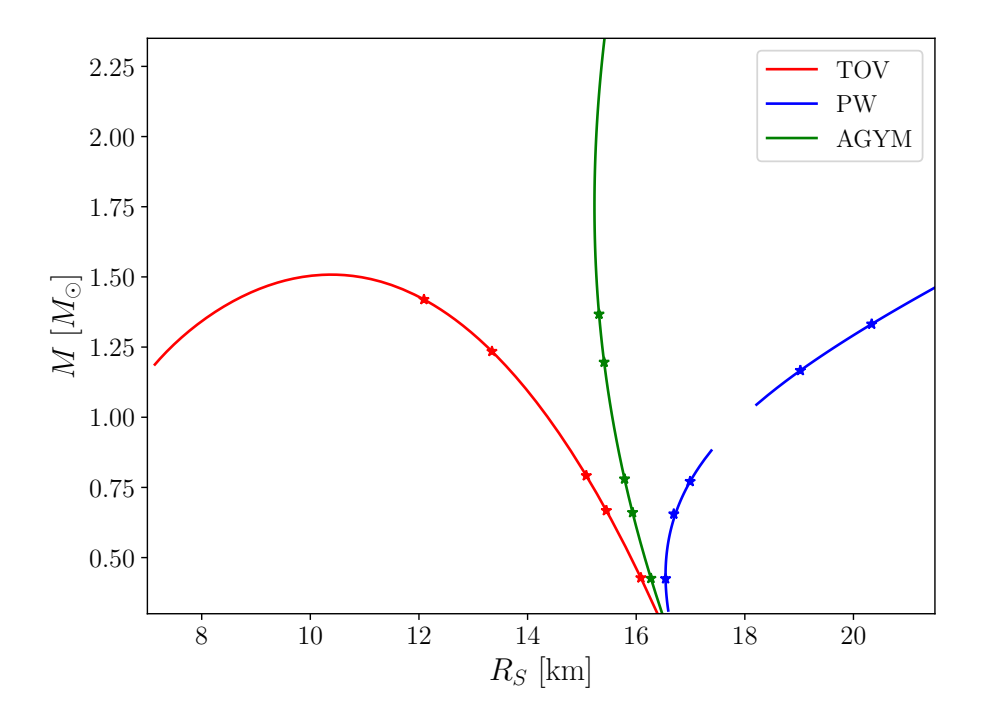


FIG. 1. Mass-radius curves for polytropic post-Newtonian stars determined from (2.6) (blue solid) and (2.11) (green solid). For comparison we also show the results for relativistic stars built by solving the Tolman-Oppenheimer-Volkoff equations (red) using the same polytropic equation of state (2.14). The gap appearing in the PW curve is the region where we would need to use higher numerical precision to determine the stellar models (for more discussion of this point, see [46]). Specific pN models considered in the mode calculations later are indicated on each respective mass-radius curve.

III. THE NON-RADIAL OSCILLATION PROBLEM

Having obtained suitable background models, we want to study non-radial perturbations and calculate the star's oscillation modes. Given the issues associated with the background configuration, this may not be entirely straightforward. With this in mind, we will pay attention to the details of each required step.

A. The perturbation equations

The derivation of the pN perturbation equations is, in principle, straightforward. As the background star is static, it is natural to work with Eulerian perturbations (the change of a physical quantity at a fixed point in space, indicated by δ) of the various thermodynamical quantities (δp , $\delta \rho$, and so on) alongside the Lagrangian displacement vector ξ^i , in our case simply given by

$$\delta v^i = \partial_t \xi^i \ . \tag{3.1}$$

Starting from the momentum equation for pN hydrodynamics, it is easy to show that the perturbations must satisfy (see [47, 48, 53])

$$\begin{split} \rho^* \left\{ \left[1 + \frac{1}{c^2} \left(\Pi + 3U + \frac{p}{\rho^*} \right) \right] \partial_t^2 \xi^i - \frac{4}{c^2} \partial_t^2 \delta V^i - \frac{1}{2c^2} \partial_t^2 \partial^i \delta X \right\} \\ + \left(1 + \frac{2U}{c^2} \right) \left(\partial^i \delta p - \frac{\delta \rho^*}{\rho^*} \partial^i p \right) - \frac{1}{c^2} \left(\delta \Pi + \frac{\delta p}{\rho^*} - \frac{p}{\rho^{*2}} \delta \rho^* \right) \partial^i p \\ - \frac{1}{c^2} \left(\partial^i p - 4 \rho^* \partial^i U \right) \delta U - \rho^* \left[1 + \frac{1}{c^2} \left(\Pi - U + \frac{p}{\rho^*} \right) \right] \partial^i \delta U - \frac{1}{c^2} \rho^* \partial^i \delta \psi = 0 \quad (3.2) \end{split}$$

along with the perturbed continuity equation

$$\delta \rho^* = -\partial_i (\rho^* \xi^i) \ . \tag{3.3}$$

The perturbations of the various potentials involved in the problem are governed by

$$\nabla^2 \delta V_i = -4\pi G \rho^* \xi_i \,\,, \tag{3.5}$$

$$\nabla^2 \delta \psi = -4\pi G \rho^* \left(-\delta U + \delta \Pi + \frac{3\delta p}{\rho^*} - 3p \frac{\delta \rho^*}{\rho^{*2}} \right) - 4\pi G \delta \rho^* \left(-U + \Pi + \frac{3p}{\rho^*} \right) , \qquad (3.6)$$

and

$$\nabla^2 \delta X = 2\delta U \ . \tag{3.7}$$

Finally, from the pN gauge condition (see [48])

$$\partial_t U + \partial_j U^j = 0 , (3.8)$$

we also have

$$\partial_t \delta U + \partial_j \delta U^j = 0 , \qquad (3.9)$$

with $\delta U^j = \partial_t \delta V^j$. This completes the set of equations we need to solve.

B. Separation of variables

In order to solve the perturbation equations, we first of all work in the frequency domain, i.e. assume that all perturbations depend on time as $e^{i\omega t}$, so that we have

$$\delta v^i = i\omega \xi^i \ . \tag{3.10}$$

Secondly, we note that the equations have been written down in Cartesian coordinates (using partial derivatives). This is, however, not a natural choice for stars; we clearly want to work in spherical coordinates and make use of angular harmonics to decouple the equations. There are two ways to effect the required change. We can either proceed in a covariant fashion, replacing partial derivatives with covariant ones and so on, or we can take a short cut. Opting for the latter (as it provides a more immediate route to the answer and also allows for a direct comparison with most of the work on the Newtonian oscillation problem, see [54]), we simply reinstate the basis vectors and write the equations as (with vectors indicated as bold)

$$-\omega^{2}\rho^{*}\left\{\left[1+\frac{1}{c^{2}}\left(\Pi+3U+\frac{p}{\rho^{*}}\right)\right]\boldsymbol{\xi}-\frac{4}{c^{2}}\delta\boldsymbol{V}-\frac{1}{2c^{2}}\boldsymbol{\nabla}\delta\boldsymbol{X}\right\}\right.$$

$$\left.+\left(1+\frac{2U}{c^{2}}\right)\left(\boldsymbol{\nabla}\delta\boldsymbol{p}-\frac{\delta\rho^{*}}{\rho^{*}}\boldsymbol{\nabla}\boldsymbol{p}\right)-\frac{1}{c^{2}}\left(\delta\Pi+\frac{\delta\boldsymbol{p}}{\rho^{*}}-\frac{p}{\rho^{*2}}\delta\rho^{*}\right)\boldsymbol{\nabla}\boldsymbol{p}\right.$$

$$\left.-\frac{1}{c^{2}}(\boldsymbol{\nabla}\boldsymbol{p}-4\rho^{*}\boldsymbol{\nabla}\boldsymbol{U})\delta\boldsymbol{U}-\rho^{*}\left[1+\frac{1}{c^{2}}\left(\Pi-\boldsymbol{U}+\frac{p}{\rho^{*}}\right)\right]\boldsymbol{\nabla}\delta\boldsymbol{U}-\frac{1}{c^{2}}\rho^{*}\boldsymbol{\nabla}\delta\psi=0\;,\quad(3.11)$$

with

$$\delta \rho^* = -\nabla \cdot (\rho^* \boldsymbol{\xi}) \tag{3.12}$$

and

$$\nabla^2 \delta V = -4\pi G \rho^* \xi \ . \tag{3.13}$$

For these equations, we have everything we need from the corresponding Newtonian problem (see, for example, the discussion in [54]), apart from the form for the Laplacian of the vector $\delta \mathbf{V}$. The missing information is, however, readily available from, for example, the viscous term in the text-book version of the Navier-Stokes equations in spherical coordinates. With this in hand, we are ready to proceed.

The next step involves expanding all scalar variables (δp , δU , $\delta \psi$, δX) in spherical harmonics Y_l^m in such a way that

$$\delta p(t, r, \theta, \phi) = e^{i\omega t} \sum_{l} \delta p_{l}(r) Y_{l}^{m}(\theta, \phi) , \qquad (3.14)$$

and similarly for the other variables. Meanwhile, we use the standard decomposition for the displacement vector $\boldsymbol{\xi}$, i.e. in an orthonormal spherical coordinate basis $(\hat{\boldsymbol{r}}, \hat{\boldsymbol{\theta}}, \hat{\boldsymbol{\phi}})$, we have

$$\boldsymbol{\xi} = \xi^r \hat{\boldsymbol{r}} + \xi^{\theta} \hat{\boldsymbol{\theta}} + \xi^{\phi} \hat{\boldsymbol{\phi}} = e^{i\omega t} \sum_{l} \left[\xi_l^r(r), \xi_l^h(r) \frac{\partial}{\partial \theta}, \xi_l^h(r) \frac{\partial}{\sin \theta \partial \phi} \right] Y_l^m(\theta, \phi) , \qquad (3.15)$$

where ξ_l^r and ξ_l^h denote the radial and tangential components, respectively. The expansion for the perturbed vector potential δV takes the same form (with components δV_l^r and δV_l^h).

Noting that we need a matter equation of state to close the system of perturbation equations and we also want to model to allow for the presence of composition gravity (g) modes, we introduce an adiabatic index Γ_1 associated with the perturbations. This assumes that the oscillations take place adiabatically and that relevant nuclear reactions are sufficiently slow that the matter composition may be considered frozen (see [55] for a recent discussion)

$$\frac{\Delta p}{p} = \Gamma_1 \frac{\Delta \rho}{\rho} \,, \tag{3.16}$$

where Δ represents a Lagrangian perturbation, which associates the small change of a quantity to a specific fluid element. This relation allows us to relate $\delta \rho_l$ to δp_l via

$$\delta \rho_l = \frac{\rho}{\Gamma_1} \frac{\delta p_l}{p} - \rho \xi_l^r A , \qquad (3.17)$$

where the Schwarzschild discriminant A takes the usual form [54]

$$A = \frac{d\ln\rho}{dr} - \frac{1}{\Gamma_1} \frac{d\ln p}{dr} \,. \tag{3.18}$$

Therefore, $\delta \rho_l^*$ can be eliminated in favour of δp using:

$$\delta \rho_l^* = \delta \rho_l \left(1 + \frac{3U}{c^2} \right) + \frac{3\rho}{c^2} \delta U_l = \frac{\rho^*}{\Gamma_1} \frac{\delta p_l}{p} - \rho^* \xi_l^r A + \frac{3\rho}{c^2} \delta U_l . \tag{3.19}$$

For the internal energy—for both barotropic and non-barotropic perturbations, see Appendix A—we have

$$\delta\Pi_l = \frac{p}{\rho^2} \delta\rho_l = \frac{p}{\rho^2} \left(\frac{\rho}{\Gamma_1} \frac{\delta p_l}{p} - \rho \xi_l^r A \right) = \frac{\delta p_l}{\Gamma_1 \rho} - \frac{p}{\rho} \xi_l^r A . \tag{3.20}$$

We proceed to split the equations of motion into radial and tangential components, using the equation of the state to eliminate $\delta \rho_l$, $\delta \rho_l^*$ and $\delta \Pi_l$. Thus, we arrive at a set of ordinary differential equations (for each l-multipole)

$$-\omega^{2}\rho^{*}\left[1+\frac{1}{c^{2}}\left(\Pi+3U+\frac{p}{\rho^{*}}\right)\right]\xi_{l}^{r}+\left(1+\frac{2U}{c^{2}}\right)A\frac{dp}{dr}\xi_{l}^{r} + \left(1+\frac{2U}{c^{2}}\right)\frac{d\delta p_{l}}{dr}-\left(1+\frac{2U}{c^{2}}\right)\frac{1}{\Gamma_{1}p}\frac{dp}{dr}\delta p_{l} - \frac{1}{c^{2}\rho^{*}}\frac{dp}{dr}\delta p_{l} - \frac{4}{c^{2}}\left(\frac{dp}{dr}-\rho^{*}\frac{dU}{dr}\right)\delta U_{l} - \rho^{*}\left[1+\frac{1}{c^{2}}\left(\Pi-U+\frac{p}{\rho^{*}}\right)\right]\frac{d\delta U_{l}}{dr} + \omega^{2}\frac{4\rho^{*}}{c^{2}}\delta V_{l}^{r} - \omega^{2}\frac{\rho^{*}}{2c^{2}}\frac{d}{dr}\delta X_{l} - \frac{1}{c^{2}}\rho^{*}\frac{d}{dr}\delta\psi_{l} = 0, \quad (3.21)$$

and

$$\omega^{2} \left[1 + \frac{1}{c^{2}} \left(\Pi + 3U + \frac{p}{\rho^{*}} \right) \right] \left\{ -\rho^{*} A \xi_{l}^{r} + \frac{d\rho^{*}}{dr} \xi_{l}^{r} + \frac{\rho^{*}}{r^{2}} \frac{d}{dr} (r^{2} \xi_{l}^{r}) \right\}$$

$$+ \omega^{2} \left[1 + \frac{1}{c^{2}} \left(\Pi + 3U + \frac{p}{\rho^{*}} \right) \right] \frac{\rho^{*}}{p \Gamma_{1}} \delta p_{l} - \left(1 + \frac{2U}{c^{2}} \right) \frac{l(l+1)}{r^{2}} \delta p_{l}$$

$$- \omega^{2} \frac{\rho^{*}}{c^{2}} \delta U_{l} + \rho^{*} \left[1 + \frac{1}{c^{2}} \left(\Pi - U + \frac{p}{\rho^{*}} \right) \right] \frac{l(l+1)}{r^{2}} \delta U_{l} - \omega^{2} \frac{4\rho^{*}}{c^{2}} \frac{1}{r^{2}} \frac{d}{dr} \left(r^{2} \delta V_{l}^{r} \right)$$

$$+ \omega^{2} \frac{\rho^{*}}{2c^{2}} \frac{l(l+1)}{r^{2}} \delta X_{l} + \frac{\rho^{*}}{c^{2}} \frac{l(l+1)}{r^{2}} \delta \psi_{l} = 0 . \quad (3.22)$$

Similarly, the perturbation equations of the potentials, obtained from (3.4)-(3.7), can be written

$$\frac{1}{r^2}\frac{d}{dr}\left(r^2\frac{d\delta U_l}{dr}\right) - \frac{l(l+1)}{r^2}\delta U_l + 4\pi G\delta\rho_l^* = 0 , \qquad (3.23)$$

$$\frac{1}{r^2} \frac{d}{dr} \left(r^2 \frac{d\delta V_l^r}{dr} \right) + \frac{2}{r} \frac{d\delta V_l^r}{dr} + \frac{2 - l(l+1)}{r^2} \delta V_l^r + \frac{2}{r} \delta U_l + 4\pi G \rho^* \xi_l^r = 0 , \qquad (3.24)$$

$$\frac{1}{r^2} \frac{d}{dr} \left(r^2 \frac{d\delta \psi_l}{dr} \right) - \frac{l(l+1)}{r^2} \delta \psi_l = -4\pi G \rho^* \left(-\delta U_l + \delta \Pi_l \right) - 4\pi G \left(3\delta p_l - 3p \frac{\delta \rho_l^*}{\rho^*} \right) - 4\pi G \delta \rho_l^* \left(-U + \Pi + \frac{3p}{\rho^*} \right) , \quad (3.25)$$

and

$$\frac{1}{r^2}\frac{d}{dr}\left(r^2\frac{d\delta X_l}{dr}\right) - \frac{l(l+1)}{r^2}\delta X_l - 2\delta U_l = 0.$$
(3.26)

In summary, we have six perturbation equations (3.21)–(3.26) for six unknown variables ξ_l^r , δp_l , δU_l , δV_l^r , $\delta \psi_l$ and δX_l . Adding the relevant boundary conditions, we can formulate an eigenvalue problem for the oscillation modes.

C. The dimensionless formulation

In order to simplify the numerical calculations it is advantageous to express the equations in dimensionless form. Following the spirit of the common formulation of the Newtonian problem (see [56]), we introduce the following dimensionless variables:

$$y_1 = \frac{\xi_l^r}{r} \,, \tag{3.27}$$

$$y_2 = \frac{1}{gr} \frac{\delta p_l}{\rho} - \left[1 + \frac{1}{c^2} \left(\Pi + \frac{p}{\rho^*} \right) \right] \frac{\delta U_l}{gr} , \qquad (3.28)$$

the definition of which serves to decouple the y_1 and y_2 pair from y_3 and y_4 . The latter are given by

$$y_3 = \frac{\delta U_l}{gr} \,, \tag{3.29}$$

$$y_4 = \frac{1}{a} \frac{d\delta U_l}{dr} \,. \tag{3.30}$$

We also introduce

$$y_5 = \frac{\delta V_l^r}{gr^2} \,, \tag{3.31}$$

$$y_6 = \frac{1}{gr} \frac{d\delta V_l^r}{dr} \,, \tag{3.32}$$

$$y_7 = \frac{\delta X_l}{gr^3} \,, \tag{3.33}$$

$$y_8 = \frac{1}{qr^2} \frac{d\delta X_l}{dr} \,, \tag{3.34}$$

$$y_9 = \frac{\delta \psi_l}{g^2 r^2} \,, \tag{3.35}$$

and

$$y_{10} = \frac{1}{g^2 r} \frac{d\delta \psi_l}{dr} \,. \tag{3.36}$$

In these relations q(r) is taken to be the local Newtonian gravitational acceleration, defined by

$$g = \frac{GM_B(r)}{r^2} \,. \tag{3.37}$$

It is worth highlighting that this scaling impacts on the radial dependence of the variables. For example, given that the potential U has the same dimensions as gr, the motivation for defining y_3 by dividing by gr instead of by U is that, near the centre of the star $gr \to \mathcal{O}(r^2)$, which helps eliminate the divergence at the centre. Another reason for working with this specific scaling¹ is that this choice facilitates direct comparison with the corresponding Newtonian problem (e.g. as described in [54]).

With the definitions of the dimensionless variables and (3.37), the six perturbation equations above (3.21)-(3.26) are reduced to ten first order differential equations for ten unknown variables. We have

$$r\frac{dy_1}{dr} = -\left(A^* + \frac{rd\rho^*}{\rho^*dr} + 3\right)y_1 - V_g y_2 + \frac{l(l+1)}{c_1\tilde{\omega}^2} \left[1 - \frac{1}{c^2} \left(\Pi + 4U + \frac{p}{\rho^*}\right)\right] y_2 - V_g \left[1 + \frac{1}{c^2} \left(\Pi + \frac{p}{\rho^*}\right)\right] y_3 + \frac{gr}{c^2} y_3 + \frac{4gr}{c^2} (2y_5 + y_6) - \frac{l(l+1)gr}{2c^2} y_7 - \frac{l(l+1)}{c^2} \frac{gr}{c_1\tilde{\omega}^2} y_9 \right], \quad (3.39)$$

$$r\frac{dy_{2}}{dr} = c_{1}\tilde{\omega}^{2} \left[1 + \frac{1}{c^{2}} \left(\Pi + 4U + \frac{p}{\rho^{*}} \right) \right] y_{1} + \frac{A^{*}}{\rho g} \frac{dp}{dr} y_{1} - \left(U_{b} - 1 - A^{*} \right) y_{2} + \frac{1}{c^{2}} \frac{dp}{dr} r y_{2}$$

$$- A^{*} \left[1 + \frac{1}{c^{2}} \left(\Pi + \frac{p}{\rho^{*}} \right) \right] y_{3} + \frac{1}{c^{2}} \left(\frac{4}{\rho} \frac{dp}{dr} - 4 \frac{dU}{dr} - \frac{d\Pi}{dr} + \frac{p}{\rho^{*2}} \frac{d\rho^{*}}{dr} \right) r y_{3}$$

$$- c_{1}\tilde{\omega}^{2} \frac{4gr}{c^{2}} y_{5} + c_{1}\tilde{\omega}^{2} \frac{gr}{2c^{2}} y_{8} + \frac{gr}{c^{2}} y_{10} , \quad (3.40)$$

$$r\frac{dy_3}{dr} = (1 - U_b)y_3 + y_4 , \qquad (3.41)$$

$$r\frac{dy_4}{dr} = -4\pi G \frac{\rho^* r}{g} (A^* y_1 + V_g y_2) - 4\pi G \frac{\rho^* r}{g} V_g \left[1 + \frac{1}{c^2} \left(\Pi + \frac{p}{\rho^*} \right) \right] y_3 - 4\pi G \frac{3\rho^* r^2}{c^2} y_3 + l(l+1)y_3 - U_b y_4 , \quad (3.42)$$

$$g_0 = \frac{4\pi}{3} G \rho_0 r \,, \tag{3.38}$$

where ρ_0 is the central mass density. This leads to a different set of dimensionless equations to solve, but the expansion near the centre remains the same. Ultimately, the strategy is a matter of choice.

¹ There are, of course, different ways one may scale the variables. For example, one could replace g(r) with a factor

$$r\frac{dy_5}{dr} = -U_b y_5 + y_6 , \qquad (3.43)$$

$$r\frac{dy_6}{dr} = -(3+U_b)y_6 - [2-l(l+1)]y_5 - 4\pi G\frac{\rho^* r}{g}y_1 - 2y_3, \qquad (3.44)$$

$$r\frac{dy_7}{dr} = -(1+U_b)y_7 + y_8 , \qquad (3.45)$$

$$r\frac{dy_8}{dr} = 2y_3 + l(l+1)y_7 - (2+U_b)y_8 , \qquad (3.46)$$

$$r\frac{dy_9}{dr} = -2(U_b - 1)y_9 + y_{10} , (3.47)$$

and

$$r\frac{dy_{10}}{dr} = -4\pi G \frac{\rho^* A^*}{g^2} \left(\frac{p}{\rho} - U + \Pi\right) y_1 - 4\pi G \left[\frac{\rho^* r}{g} \frac{1}{\Gamma_1} + \frac{3\rho r}{g} - \frac{\rho^*}{g^2} (U - \Pi) V_g\right] y_2$$

$$+ 4\pi G \frac{r}{g} \left[\rho^* + \frac{3\rho}{c^2} (U - \Pi)\right] y_3 - 4\pi G \left[\frac{\rho^* r}{g} \frac{1}{\Gamma_1} + \frac{3\rho r}{g} - \frac{\rho^*}{g^2} (U - \Pi) V_g\right] \left[1 + \frac{1}{c^2} \left(\Pi + \frac{p}{\rho^*}\right)\right] y_3$$

$$+ l(l+1)y_9 + (1-2U_b) y_{10} . \quad (3.48)$$

In these equations we have used the additional definitions (again, similar to the Newtonian problem [54]):

$$A^* = -rA = -\frac{rd\rho}{\rho dr} + \frac{r}{p\Gamma_1} \frac{dp}{dr}, \qquad (3.49)$$

$$V_g = \frac{\rho g r}{\Gamma_1 p} \,, \tag{3.50}$$

$$U_b = \frac{d \ln M_B(r)}{d \ln r} = \frac{4\pi \rho^* r^3}{M_B(r)} = \frac{r \, dg}{q \, dr} + 2 \,\,, \tag{3.51}$$

$$c_1 = \left(\frac{r}{R}\right)^3 \frac{M}{M_B(r)} \,. \tag{3.52}$$

We have also introduced the dimensionless frequency

$$\tilde{\omega}^2 = \frac{\omega^2 R^3}{GM} \,. \tag{3.53}$$

With these variables, the dimensionless formulation of the equations is complete.

D. The boundary conditions

Complemented by the appropriate boundary conditions at the centre and the surface of the star, the oscillation equations form an eigenvalue problem. The conditions we need to impose are natural extensions of the usual ones: First, we need the physical solution to be regular at the centre of the star. Second, at the star's surface we need the Lagrangian perturbation of the pressure to vanish while the potentials δU_l , δX_l , δV_l^r and $\delta \psi_l$ and their derivatives are continuous across r = R.

The analysis of the solution at the centre of the star involves a Taylor expansion. In fact, in order to avoid numerical difficulties, the integration of the equations is always initiated a small distance $r = r_{\epsilon}$ away from the origin. Adapting the strategy used in [54], we express the problem as a matrix problem

$$r\frac{dy_k}{dr} = \bar{A}_{kl}y_l \tag{3.54}$$

where the matrix \bar{A}_{lk} (provided in Appendix B) represents the central values (actually, at r_{ϵ}) of the various coefficients from the (dimensionless) perturbation equations. Then solving the characteristic equation

$$\det(\bar{A}_{ij} - \lambda \delta_{ij}) = 0 , \qquad (3.55)$$

where the δ_{ij} is the Kronecker delta, we arrive at a set of eigenvalues λ_i and the corresponding eigenvectors Y_i constructed from the solutions $y_1 - y_{10}$. Rejecting the singular solutions and combining the remaining ones one finds that (again, see Appendix B for details) the following five conditions must be satisfied at the centre of the star:

$$y_2 - \frac{1+l}{a}y_1 = 0 , (3.56)$$

$$y_4 - ly_3 = 0 (3.57)$$

$$y_6 - (l-1)y_5 + \frac{3y_1 + 2y_3}{3+2l} = 0 , (3.58)$$

$$y_8 - ly_7 - \frac{2y_3}{3+2l} = 0 , (3.59)$$

and

$$y_{10} - ly_9 - \frac{ae + (l+1)f}{a(3+2l)}y_1 - \frac{\bar{g}}{3+2l}y_3 = 0.$$
(3.60)

Here we have defined (the subscript 0 indicates the central value of each quantity)

$$a = \frac{l(l+1)}{\omega^2} \frac{4\pi}{3} G \rho_0^* \left[1 - \frac{1}{c^2} \left(\Pi_0 + 4U_0 + \frac{p_0}{\rho_0^*} \right) \right] , \qquad (3.61)$$

$$c = \frac{3\omega^2}{4\pi G \rho_0^*} \left[1 + \frac{1}{c^2} \left(\Pi_0 + 4U_0 + \frac{p_0}{\rho^* 0} \right) \right] , \qquad (3.62)$$

$$e = \left(U_0 - \Pi_0 - \frac{p_0}{\rho_0}\right) \frac{9}{2\pi G \rho_0^*} \left(\frac{p_2}{p_0 \Gamma_1} - \frac{\rho_2}{\rho_0}\right) , \qquad (3.63)$$

$$f = (U_0 - \Pi_0) \frac{3}{\Gamma_1} \frac{\rho_0}{\rho_0} - \frac{3}{\Gamma_1} - 9\left(1 - \frac{3U_0}{c^2}\right) , \qquad (3.64)$$

and

$$\bar{g} = 3\left[1 + \frac{3}{c^2}(U_0 - \Pi_0)\right] - 3\left[\frac{1}{\Gamma_1} + \frac{3\rho_0}{\rho_0^*} - (U_0 - \Pi_0)\frac{\rho_0}{p_0\Gamma_1}\right]\left[1 + \frac{1}{c^2}\left(\Pi_0 + \frac{p_0}{\rho_0^*}\right)\right] . \tag{3.65}$$

For realistic matter models, we should Taylor expand Γ_1 as well, but here we will only consider the simplified case where Γ_1 is a constant.

Moving on to the behaviour at the stellar surface, we need another five conditions to be satisfied. The first of these conditions involves the vanishing of the Lagrangian pressure perturbation, $\Delta p = 0$. That is, we have

$$\Delta p_l = \delta p_l + \xi_l^r \frac{dp}{dr} = 0 \ . \tag{3.66}$$

In the case of the PW scheme the pressure gradient follows from (2.6) and (similar to the definition of g) we define

$$g_1 = \frac{G\mathcal{N}}{r^2} \,, \tag{3.67}$$

to arrive at

$$y_2 + \left[1 + \frac{1}{c^2} \left(\Pi + \frac{p}{\rho^*}\right)\right] y_3 = y_1 \left\{ \left[1 + \frac{1}{c^2} \left(\Pi - 3U + \frac{p}{\rho^*}\right)\right] + \frac{1}{c^2} \frac{g_1}{g} \right\} \frac{\rho^*}{\rho}.$$
 (3.68)

Given that Π , ρ and p vanish at the surface (for the stellar models we consider), we obtain a boundary condition constraining y_1 and y_2 :

$$y_2 = -y_3 + y_1 \left(1 - \frac{3U}{c^2} + \frac{1}{c^2} \frac{g_1}{g} \right) \left(1 + \frac{3U}{c^2} \right)$$
 at $r = R$. (3.69)

For the AGYM model, the equation for hydrostatic equilibrium is different and the boundary condition for y_1 and y_2 changes slightly. In this case we have:

$$y_2 = -y_3 + y_1 \left(1 + \frac{g_1}{g}\right)$$
 at $r = R$. (3.70)

In both cases, we also need to ensure the continuity of the four perturbed potentials $\delta U, \delta V, \delta X$ and $\delta \psi$ and their derivatives across the surface. As discussed in Appendix B, this leads to the surface relations

$$y_4 + (l+1)y_3 = 0 (3.71)$$

$$(l+2)y_5 + y_6 - \frac{2y_3}{2l-1} = 0 , (3.72)$$

$$(l+1)y_7 + y_8 + \frac{2}{2l-1}y_3 = 0 , (3.73)$$

and

$$y_{10} + (l+1)y_9 = 0. (3.74)$$

We now have all the conditions we need to impose in order to determine the required mode solutions. We may proceed to discuss the numerical results.

IV. NUMERICAL RESULTS

The ten first order differential equations and ten boundary conditions together form an eigenvalue problem for the oscillation frequencies we want to determine. In order to solve the problem numerically, we adapt the strategy from the relativistic problem, see for instance [39, 57]. Schematically, this involves integrating five linearly independent solutions that satisfy the conditions at the centre of the star (see Appendix B) and matching them to a set of five solutions obtained by integration backwards from the stellar surface (where they satisfy the required conditions, again discussed in Appendix B). Formally, representing the solution to the system of equations (3.39)-(3.48) by $\mathcal{Y}(r) = [y_1, y_2, ..., y_{10}]^T$, we have

$$r\frac{d}{dr}\mathcal{Y} = \bar{A}\mathcal{Y} \ . \tag{4.1}$$

The boundary conditions at the centre provide five linearly independent vectors \mathcal{Y}_i^c (with i = 1 - 5) and the linear combination

$$\mathcal{Y}_c = \sum_{i=1}^5 a_i \mathcal{Y}_i^c , \qquad (4.2)$$

then provides the general solution. The coefficients a_i are yet to be determined. Similarly, the solution that satisfies the required conditions at the surface can be expressed in terms of \mathcal{Y}_i^s (with i = 6 - 10) each of which satisfies the boundary conditions at the surface. The corresponding solution then takes the form

$$\mathcal{Y}_s = \sum_{i=6}^{10} a_i \mathcal{Y}_i^s \ . \tag{4.3}$$

Finally, the constant coefficients are determined by matching the two solutions at r_m , a suitable point inside the star. Choosing to match at the middle of the star $(r_m = R/2)$, we simply require

$$\mathcal{Y}_c(R/2) = \mathcal{Y}_s(R/2) . \tag{4.4}$$

As discussed in, for example, [58] the matching condition can be turned into the requirement that the determinant constructed from the numerical solution vectors must vanish. This then leads to the condition for the eigenvalues

$$\det \left[\mathcal{Y}_{1}^{c}, \mathcal{Y}_{2}^{c}, \mathcal{Y}_{3}^{c}, \mathcal{Y}_{4}^{c}, \mathcal{Y}_{5}^{c}, -\mathcal{Y}_{6}^{s}, -\mathcal{Y}_{7}^{s}, -\mathcal{Y}_{8}^{s}, -\mathcal{Y}_{9}^{s}, -\mathcal{Y}_{10}^{s} \right] = \mathcal{D}(\tilde{\omega}) = 0 \ . \tag{4.5}$$

The values of $\tilde{\omega} = \tilde{\omega}_n$ for which the determinant vanishes are the mode frequencies. For each $\tilde{\omega}_n$ we can work out the eigenfunctions by solving (4.4) for $a_1 - a_{10}$. A sample of mode eigenfunctions are provided in Figure 2.

In order to explore how the pN scheme performs, let us first consider three models with the relatively low baryon masses $M_B = 0.436 M_{\odot}, 0.669 M_{\odot}$ and $0.823 M_{\odot}$. A sample of numerical results is provided in Table I. As the table shows, we have calculated the fundamental f-mode and the lowest order p-modes and g-modes for a $\Gamma=2$ polytropic background model with constant adiabatic index $\Gamma_1 = 2.1$ for the perturbations. The details of the model are, however, not that important. The key points we want to stress here relate to the comparison of the different formulations of the problem. Specifically, Table I provides results obtained for both background models. The data clearly bring out the expectation that the two models lead to similar results for low-mass stars. After all, in the weak-field limit the post-Newtonian corrections should be small. The numerical results also show that the mode frequencies tend to decrease when the gravitational redshift is accounted for, an effect that increases for more compact stars. Adding to this, we know from the mass-radius curves in Figure 1 that, for a given mass the two pN models differ substantially in the stellar radius. The difference increases as the stars become heavier. This highlights an obvious problem with this kind of comparison. In addition, the scaling of the frequency with the radius is problematic. In the pN scheme, the calculation is carried out using isotropic coordinates, while it is more common to solve the relativistic problem in Schwarzschild coordinates. In the Newtonian limit, this makes no difference but for heavier stars we need to pay attention to this. At the end of the day, these caveats suggest that the actual values for the frequencies provided in Table I are less important than the trends in the results. The most important lessons are i) that the calculation can be carried out and the mode results for low-mass stars are sensible (including the eigenfunctions, see the example provided in Figure 2), but ii) the calculation unfortunately breaks for more massive stars.

	Newtonian	\mathbf{PW}	AGYM	\mathbf{PW}	AGYM	\mathbf{PW}	AGYM
$M_{ m B}/M_{\odot}$		0.4361	0.4363	0.6689	0.6689	0.8231	0.8232
M/M_{\odot}		0.4247	0.4259	0.6374	0.6419	0.7712	0.8016
$R_{\rm S}/{ m km}$		16.5407	16.2712	16.6919	15.9570	16.9930	15.5085
p_3	7.4590	6.6291	6.7912	6.1016	6.4214	5.7251	5.9672
p_2	5.5743	4.9539	5.0775	4.5522	4.7951	4.2630	4.4461
p_1	3.5785	3.1849	3.2694	2.9211	3.0887	2.7291	2.8676
f	1.2277	1.1232	1.1673	1.0267	1.1237	0.9497	1.0756
g_1	0.2566	0.2314	0.2406	0.2100	0.2304	0.1933	0.2165
g_2	0.1770	0.1582	0.1646	0.1417	0.1557	0.1288	0.1439

TABLE I. The dimensionless quadrupole (l=2) oscillation frequencies $\tilde{\omega}_n$ for our baseline polytropic model with $\Gamma=2$, $K=185~{\rm km}^2$ and $\Gamma_1=2.1$. The numerical data bring out the expectation that the two pN models (PW and AGYM) agree well in the weak-field regime but, as the stellar radius corresponding to the same (baryon) mass begin to differ for more massive stars, the mode results also begin to diverge. The general trend observed in the results makes sense given that the mode frequencies are expected to decrease compared to the Newtonian case because of the gravitational redshift.

The problems associated with the pN scheme become apparent when we consider heavier (and hence more realistic) neutron star models. We know already from Figure 1 that the divergence of the PW scheme away from the fully relativistic background models is much more drastic than for the AGYM models, but it is obviously the case that

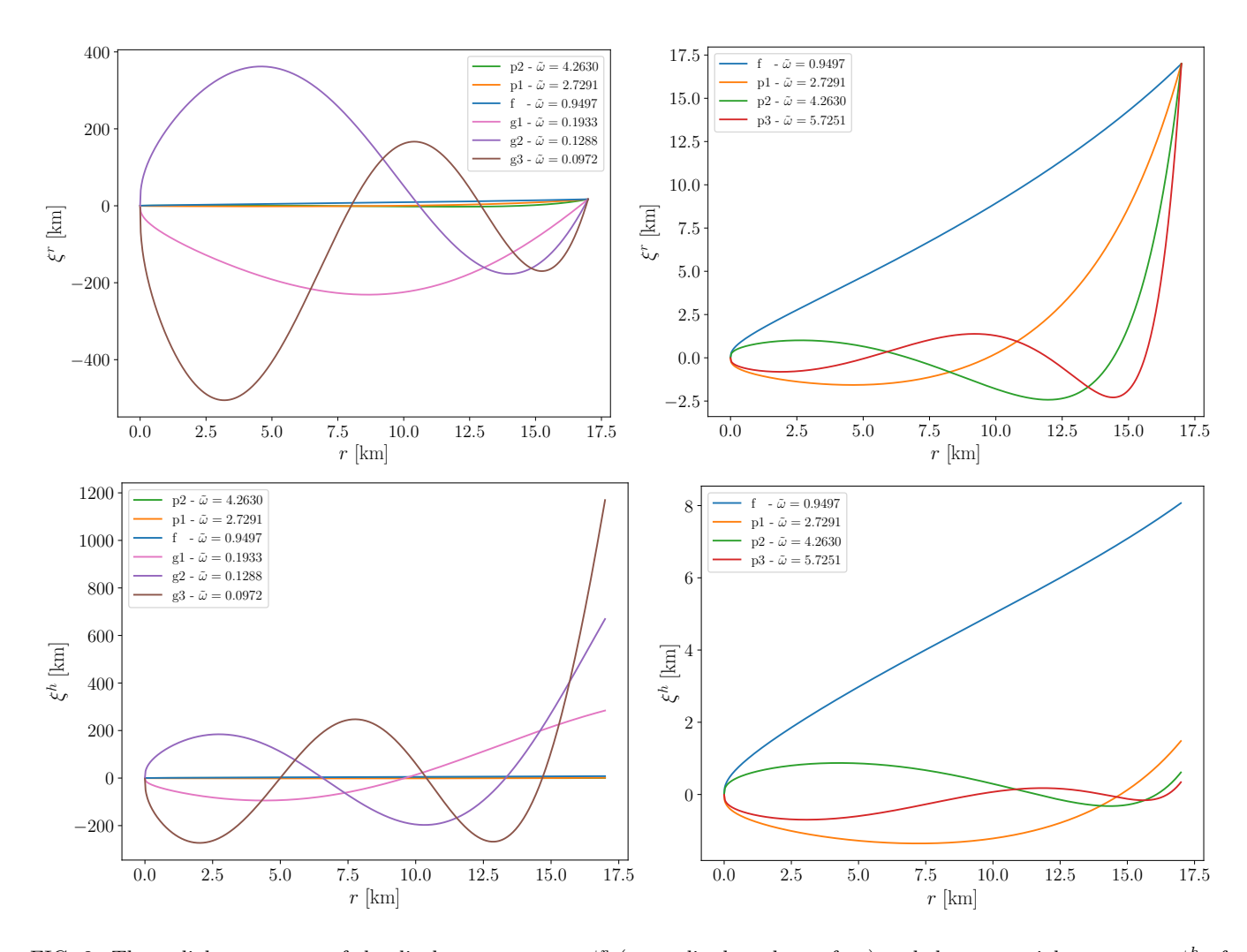


FIG. 2. The radial component of the displacement vector ξ^r (normalised at the surface) and the tangential component ξ^h of f, p_1, p_2, g_1, g_2 and g_3 modes of a static star with gravitational mass of $0.771 M_{\odot}$, built with the PW scheme. These solutions are indicative of the behaviour found for low-mass stars in both pN formulations.

the error in the stellar radius is substantial for both schemes once we consider stars above $M_B \approx 1 M_{\odot}$. This is not surprising as these stars are in the strong-gravity regime and one would intuitively expect the pN approach to break down. This is, indeed, what happens. However, it is interesting to note how and why the calculation breaks. We get an immediate clue to the answer from the results for a model with $M_B = 1.322 M_{\odot}$. In this case, the eigenvalue calculation appears to proceed without a hitch, but when we consider the mode eigenfunctions we note that they are no longer well behaved near the origin. Specifically, the radial component of the displacement vector ξ_r diverges at the centre. This behaviour can be understood from the discussion following equation (B30) in Appendix B. Specifically, if the central value of the gravitational potential, U_0 , becomes too large then the Taylor expansion no longer provides a well-behaved solution. Evidence that this, indeed, happens is provided in Figure 3. Once the value of U_0 exceeds 1/4 once would expect the calculation to be come problematic and this is exactly what we find. Again, it might be tempting to argue that this was entirely expected and that we do not learn very much from this exercise. This may be true, but we suggest that it is nevertheless useful to make the result quantitative. It is now much clearer how the pN approach does not just become less accurate, it breaks completely for realistic neutron star parameters.

Having identified the problem—or at least the most pressing one—we can also ask if we can adjust the calculation to do better. We will, indeed, suggest a strategy that would be helpful in this respect, but before doing so we should acknowledge that this involves abandoning that logic of the pN expansion. This inevitably involves a different set of choices and we are not going to claim anything other than that our adapted strategy provides a pragmatic way to circumvent the numerical problem we have identified. Schematically, noting that the divergence in the eigenfunctions appears near the origin, we consider what happens if we retain higher order pN terms in the small r expansion. After all, the results in Figure 3 clearly show that we cannot safely neglect the higher order terms involving the gravitational

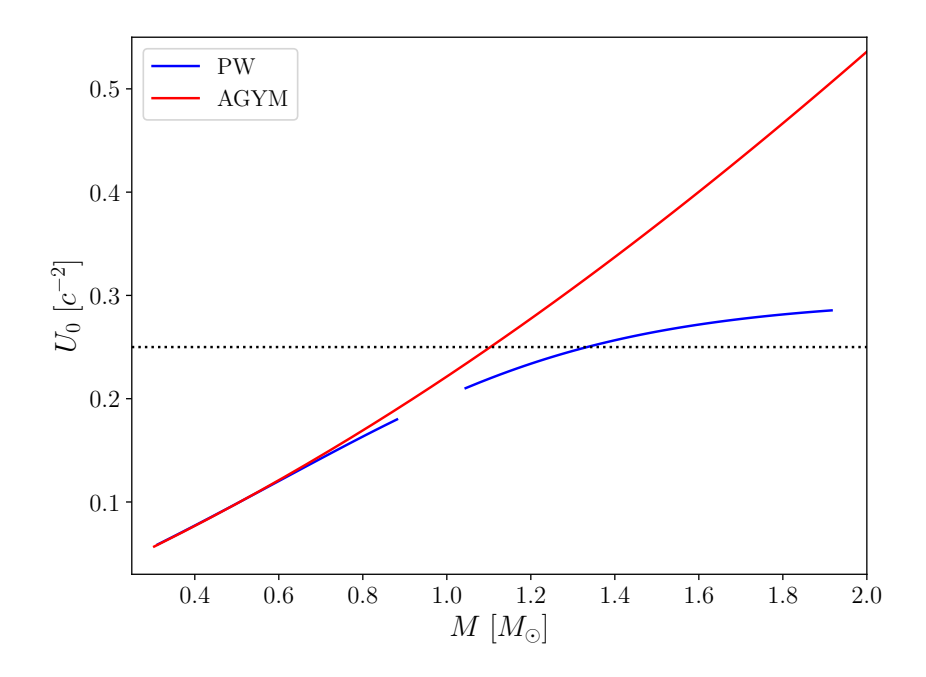


FIG. 3. The variation of the central value of the potential U_0 with the gravitational mass M for stars built within the two pN schemes (2.6) (blue solid) and (2.11) (red solid) for the same polytropic equation of state as in Table I.

potential. One way to deal with this problem, inspired by discussion in [46, 59], is outlined in Appendix C. The argument proceeds as follows: In the steps going from (3.21) to (3.40), we multiplied by

$$\frac{1}{\rho g} \left(1 - \frac{2U}{c^2} \right) ,$$

expanded the result and kept only the 1pN terms. For example, we had

$$\left(1 - \frac{2U}{c^2}\right) \times \left(1 + \frac{2U}{c^2}\right) A \frac{dp}{dr} r y_1 = \left(1 - \frac{4U^2}{c^4}\right) A \frac{dp}{dr} r y_1 \approx A \frac{dp}{dr} r y_1.$$

This simplification is evidently not valid in the neutron star regime, when the contribution from U^2/c^4 can no longer be ignored. A simple alternative would be, rather than expanding, to simply divide by the term including the gravitational potential. This leads to equations (C1) and (C2) for y_2 and y_1 , respectively. Replacing these two equations, we find that we are able extend the mode calculation to heavier masses without encountering any problems at the origin. Typical results obtained with this approach are provided in Table II. The models presented in the Table are indicated on the respective mass-radius curves in Figure 1.

The new set of results extend the calculation into the neutron-star mass range. Comparing to the data in Table I, we learn that the reformulation of the equations (evidently including higher order pN terms in a different way) lead to slightly higher frequencies for all modes. This effect becomes more pronounced for more massive stars, as one might expect given that the higher order pN terms play a more important role. Comparing the results for the PW and AGYM models we also see that—as expected, given the divergence of the two mass-radius curves, see Figure 1—the mode results for the PW model change sharply once the stellar mass is increased above $1M_{\odot}$.

So far, we have mainly compared the two pN models to the Newtonian results. Given that the mode problem was formulated in a way that resembles the Newtonian problem (see, in particular, [54]) it made sense to make this comparison. Of course, the real test of the pN calculation must be a comparison to the fully relativistic problem. Having established that the calculation can be carried out for realistic neutron star masses, let us turn to this comparison. For this exercise we will no longer consider the dimensionless frequency $\tilde{\omega}$. Instead, as we do not want to bias the result by scaling with the radius (which we anyway know differs from the solution to the relativistic structure equations) we will consider the actual dimensional frequency $\omega/2\pi$ in kHz and a dimensionless representation $\bar{\omega} = GM\omega/c^3$ based on a scaling with the gravitational mass. We will also compare to results obtained within the

	Newtonian	\mathbf{PW}	AGYM	\mathbf{PW}	AGYM	\mathbf{PW}	AGYM	\mathbf{PW}	AGYM	PW	AGYM
$M_{ m B}/M_{\odot}$		0.4361	0.4363	0.6892	0.6892	0.8231	0.8232	1.3223	1.3224	1.5469	1.5469
M/M_{\odot}		0.4247	0.4259	0.6554	0.6604	0.7712	0.7801	1.1666	1.1961	1.3319	1.3674
$R_{\rm S}/{ m km}$		16.5407	16.2712	16.7222	15.9328	16.9930	15.7854	19.0227	15.4093	20.3351	15.3157
p_3	7.4590	6.6881	6.8521	6.2115	6.5669	5.9567	6.4347	5.0484	6.0446	4.6819	5.9145
p_2	5.5743	5.0036	5.1288	4.6481	4.9193	4.4574	4.8222	3.7755	4.5369	3.4998	4.4424
p_1	3.5785	3.2209	3.3064	2.9916	3.1787	2.8667	3.1198	2.4109	2.9484	2.2237	2.8930
f	1.2277	1.1376	1.1821	1.0522	1.1597	0.9968	1.1491	0.7376	1.1824	0.5984	1.1083
g_1	0.2566	0.2342	0.2434	0.2146	0.2373	0.2023	0.2345	0.1512	0.2268	0.1282	0.2245
g_2	0.1770	0.1611	0.1677	0.1472	0.1635	0.1385	0.1617	0.1024	0.1568	0.0867	0.1555
g_3	0.1360	0.1238	0.1289	0.1130	0.1257	0.1062	0.1243	0.0779	0.1206	0.0659	0.1197

TABLE II. The dimensionless mode oscillation frequencies $\tilde{\omega}_n$ for the reformulated pN problem. The stellar models are the same as in Table I.

relativistic Cowling approximation (where the perturbations of the spacetime metric, and hence the gravitational-wave aspects, are ignored). The corresponding results are obtained from the numerical code described in [60]. Moreover, we will focus our attention on the results for the fundamental f-mode within the AGYM prescription. This is, after all, the "best performing" out of the pN frameworks we have considered. The relevant results are provided in Table III. The corresponding PW results are included in Figure 4. The picture that emerges is this: The pN calculation provides very accurate results for low-mass stars. It is notably more precise than the relativistic Cowling calculation in this regime. The latter overestimates the fundamental mode frequencies by 15-20% across the entire mass range we have considered. Having said that, for stellar masses above about $1M_{\odot}$ the pN results become less accurate. For the most massive star we consider here $(M_B \approx 1.54 M_{\odot})$ the error in the pN mode frequency is similar to that of the Cowling calculation. However, while the latter overestimates the frequency, the pN calculation underestimates it. The overall behaviour is nicely represented by Figure 4. The result suggest that, for low-mass neutron stars the pN scheme performs quite well. This, in turn, lends support for a future effort to complete a pN model for dynamics tides in binary systems. It is worth to mention that, for the $0.823M_{\odot}$ stars, the background AGYM stellar model shows a difference of 0.7km from the TOV model, while both f mode frequencies are quite close to the fully relativistic results, which looks suspicious. There are many factors (the whole background configurations) entering the calculations of frequencies, it is hard to track strictly how each factor affects the final results. However, we may be able to comment on an overall effect, in the lower mass region, the post-Newtonian approximation is good enough to get both frequencies (whether scaling over the background mass and radius or not) close to the fully relativistic results.

	TOV	AGYM	TOV	AGYM	TOV	AGYM	TOV	AGYM	TOV	AGYM
$M_{ m B}/M_{\odot}$	0.4365	0.4363	0.6895	0.6892	0.8234	0.8234	1.3223	1.3224	1.5469	1.5469
M/M_{\odot}	0.4279	0.4259	0.6675	0.6604	0.7917	0.7801	1.2346	1.1961	1.4214	1.3674
$R_{ m S}/{ m km}$	16.0855	16.2712	15.4505	15.9328	15.0812	15.7854	13.3438	15.4093	12.0714	15.3157
$(\omega_f/2\pi)/\mathrm{kHz}$	0.7248	0.7234	0.9609	0.9460	1.0861	1.0537	1.6226	1.4160	2.0089	1.5633
Cowling	0.9478	-	1.2332	-	1.3767	-	1.9546	-	2.3394	-
$\bar{\omega}_{m{f}}$	0.009599	0.009535	0.01985	0.01933	0.02661	0.02544	0.06200	0.07898	0.08837	0.06615
Cowling	0.01255	-	0.02548	-	0.03373	-	0.07468	-	0.1029	-

TABLE III. Comparing pN results for the fundamental mode (obtained from the AGYM formulation of the problem) to the fully relativistic results and results obtained within the relativistic Cowling approximation. The pN models and the relativistic stars have the same baryon mass and hence can be considered to represent the "same star" in different representations of gravity.

V. CONCLUDING REMARKS

With the aim of (eventually) describing the dynamical tides in binary neutron star systems using a post-Newtonian mode-sum approach, we have developed a pN perturbation formalism for the required neutron star dynamics. We kept the computation to 1pN order, no tails effect is included, the oscillation problem stays Hermitian, the modes remain complete. The results we have provided convey a simple message: the pN formalism becomes less robust as the star

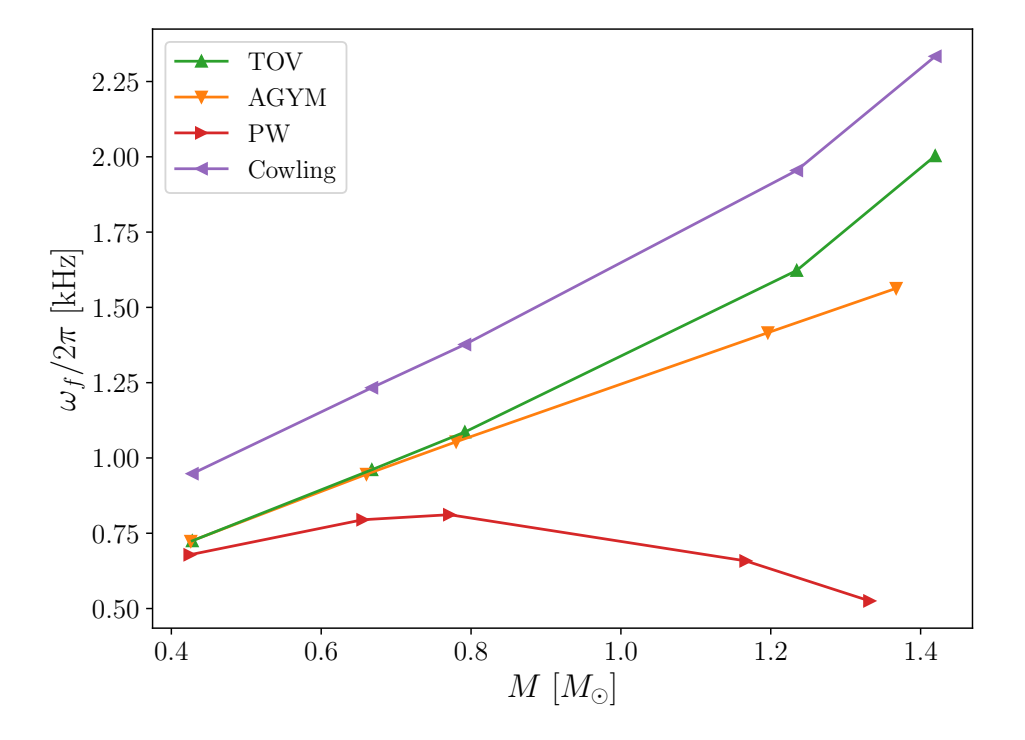


FIG. 4. The f-mode frequencies $\omega_f/2\pi$ from Table III shown as functions of the gravitational mass M of the star. Here we also include results obtained within the PW formulation of the pN problem.

becomes more compact. While it would be fair to suggest that this was expected—after all, the pN approximation assumes that the matter involves slow motion, low pressures and a weak gravitational field, assumptions not relevant for neutron stars—there are important lessons to learn from the precise way in which the calculation breaks down. As our results demonstrate, the problem involves a number of subtle issues that warrant detailed investigation. Moreover, it is possible to tweak the formulation to avoid some of the numerical issues that arise.

As a positive note, our results show (see for example Figure 4) how accurate the pN model is for lighter stars. In fact, the results demonstrate that the model remains useful up to a neutron star mass of about $1M_{\odot}$. We have also demonstrated that the pN calculation is much more accurate than the relativistic Cowling approximation in this regime. This is, however, no longer the case for canonical $1.4M_{\odot}$ neutron stars, for which the error in the pN mode frequency is comparable to that of the Cowling calculation. The main take-home message is that a pN model provides a very accurate description for the dynamics of mildly relativistic systems (e.g. white dwarf oscillation modes, tides etcetera) and may provide useful insights into the dynamics of low-mass neutron stars, as well.

Having carried out this investigation, we have a much better understanding of how the various weak-field assumptions associated with pN theory impact on the problem of stellar oscillations. While we started with an intuitive idea of the problem, we now have a quantitative picture. Specifically, we know at what point the pN background model becomes dubious and how this breakdown influences the dynamics at the linear perturbation level. With a more precise knowledge of the limitations of—and conceptual challenges associated with—the pN approach, we may consider future applications, like the development of a mode-sum approach for dynamical tides, with open eyes.

DATA AVAILABILITY STATEMENT

The data that support the findings of this study are available on Zenodo [61].

ACKNOWLEDGMENTS

SY wish to thank Rhys Counsell and David Trestini for helpful discussions. NA gratefully acknowledges support from the STFC via grant No. ST/Y00082X/1. FG acknowledges funding from the European Union's Horizon Europe research and innovation programme under the Marie Skłodowska-Curie grant agreement No. 101151301.

Appendix A: Thermodynamical relations

In this Appendix we show that equation (3.20), which is used to express the perturbed internal energy, holds for both barotropic and non-barotropic (frozen composition) models.

Let us first consider the barotropic case. For a single fluid, with $\varepsilon = \varepsilon(n)$, the usual Gibbs relation leads to

$$p + \varepsilon = n \frac{d\varepsilon}{dn} \,, \tag{A1}$$

where n is the baryon number density. Introducing the (baryon) mass density, $\rho = mn$ (with m the rest mass of each baryon), we therefore have

$$\frac{d\varepsilon}{d\rho} = \frac{p+\varepsilon}{\rho} \,. \tag{A2}$$

In the pN problem we introduced the internal energy per unit mass Π through (2.1). This means that (A2) leads to

$$d\Pi - \frac{p}{\rho^2}d\rho = 0. (A3)$$

The same relation holds for Eulerian perturbations, so we have the required result:

$$\delta\Pi = \frac{p}{\rho^2}\delta\rho \ . \tag{A4}$$

The non-barotropic case is a little bit more involved. Assuming that the matter is cold enough that we can ignore thermal effects, we start from a two-parameter equation of state, say $\varepsilon = \varepsilon(n, x_{\rm p})$, where the second parameter is the proton fraction $x_{\rm p}$. In general, we need to account for nuclear reactions [55, 62]. For an npe (neutrons, protons and electrons) system we have

$$p + \varepsilon = n_{\rm n}\mu_{\rm n} + n_{\rm p}\mu_{\rm p} + n_{\rm e}\mu_{\rm e} , \qquad (A5)$$

where each chemical potential μ_x with x = n, p, e, is defined by

$$\mu_{\mathbf{x}} = \frac{\partial \varepsilon}{\partial n_{\mathbf{x}}} \quad . \tag{A6}$$

For the equilibrium configuration, we impose beta-equilibrium which means that

$$\mu_{\rm n} = \mu_{\rm p} + \mu_{\rm e} \ . \tag{A7}$$

We also require local charge neutrality, so

$$n_{\rm p} = n_{\rm e} \ . \tag{A8}$$

Imposing the latter condition and introducing the baryon number density $n = n_{\rm n} + n_{\rm p}$ we have

$$p + \varepsilon = n\mu_{\rm n} + nx_{\rm p}(\mu_{\rm p} + \mu_{\rm e} - \mu_{\rm n}) , \qquad (A9)$$

which, in equilibrium, leads back to (A1) once we identify $\mu = \mu_n(n)$. Similarly, a variation of the energy gives (in terms of ρ rather than n)

$$d\varepsilon = \frac{1}{m} \left[(1 - x_{\rm p})\mu_{\rm n} + x_{\rm p}(\mu_{\rm p} + \mu_{\rm e}) \right] d\rho + \frac{\rho}{m} (\mu_{\rm p} + \mu_{\rm e} - \mu_{\rm n}) dx_{\rm p} . \tag{A10}$$

Meanwhile, from the form of the energy assumed in the pN calculation (2.1) we should have

$$d\varepsilon = (c^2 + \Pi)d\rho + \rho \left(\frac{\partial \Pi}{\partial \rho}\right)_{x_{\rm p}} d\rho + \rho \left(\frac{\partial \Pi}{\partial x_{\rm p}}\right)_{\rho} dx_{\rm p} . \tag{A11}$$

We are interested in frozen composition—i.e., assume that nuclear reactions are too slow to equilibrate that matter on the timescale associated with the dynamics—which means that the variations ensure that $dx_p = 0$. Assuming that the background model is in chemical equilibrium, we then arrive at the relation

$$\left(\frac{\partial\Pi}{\partial\rho}\right)_{x_{\rm p}} = \frac{p}{\rho^2} \ . \tag{A12}$$

In order to tie everything together, consider Lagrangian perturbations for which we have

$$\Delta p = \left(\frac{\partial p}{\partial \rho}\right)_{x_{\rm p}} \Delta \rho + \left(\frac{\partial p}{\partial x_{\rm p}}\right)_{\rho} \Delta x_{\rm p} . \tag{A13}$$

Provided the nuclear reactions are slow enough, we assume the composition to be frozen, so $\Delta x_p = 0$ and

$$\Delta p = \left(\frac{\partial p}{\partial \rho}\right)_{x_{\rm D}} \Delta \rho \equiv \frac{p\Gamma_1}{\rho} \Delta \rho \ . \tag{A14}$$

This provides the thermodynamical definition for the adiabatic index Γ_1 . For the Eulerian perturbations, it follows that

$$\delta p = \frac{p\Gamma_1}{\rho} \delta \rho + \left(\frac{p\Gamma_1}{\rho} \xi^i \partial_i \rho - \xi^i \partial_i p \right) , \qquad (A15)$$

In terms of the internal energy, with frozen composition, we must have

$$\Delta\Pi = \left(\frac{\partial\Pi}{\partial\rho}\right)_{x_{\rm D}} \Delta\rho , \qquad (A16)$$

so

$$\delta\Pi = \left(\frac{\partial\Pi}{\partial\rho}\right)_{x_{\rm p}}\delta\rho + \left[\left(\frac{\partial\Pi}{\partial\rho}\right)_{x_{\rm p}}\xi^{i}\partial_{i}\rho - \xi^{i}\partial_{i}\Pi\right] = \left(\frac{\partial\Pi}{\partial\rho}\right)_{x_{\rm p}}\delta\rho + \left[\left(\frac{\partial\Pi}{\partial\rho}\right)_{x_{\rm p}} - \frac{p}{\rho^{2}}\right]\xi^{i}\partial_{i}\rho , \qquad (A17)$$

which is consistent with the barotropic result. Finally, making use of (A12) we arrive at

$$\delta \Pi = \frac{p}{\rho^2} \delta \rho , \qquad (A18)$$

which is equation (3.20) from the main body of the paper.

Appendix B: Boundary conditions

1. At the centre of the star

In order to work out the required boundary conditions at the centre of the star—essentially, imposing regularity of the perturbations—we make use of a Taylor expansion. For the background quantities, this means that we have (at an initial point $r = r_{\epsilon}$ near the centre)

$$p = p_0 + p_2 r^2 + \dots$$
, $\rho = \rho_0 + \rho_2 r^2 + \dots$

We also know that, for the polytropic model we are working with we have

$$p_0 = K\rho_0^2$$
 and $p_2 = 2K\rho_2 p_0$. (B1)

It is straightforward to work out the corresponding behaviour of the centre for all other background quantities. For example, one finds that

$$p_2 = -G\frac{2\pi}{3}\rho_0^{*2} \left[1 + \frac{2}{c^2} \left(\Pi_0 - 2U_0 + \frac{3p_0}{\rho_0^*} \right) \right] , \tag{B2}$$

with

$$\rho_0^* = \rho_0 \left(1 + \frac{3U_0}{c^2} \right) . \tag{B3}$$

The analysis of the perturbation equations is more involved. Expressing the set of equations as a matrix problem

$$r\frac{dy_k}{dr} = \bar{A}_{kl}y_l , \qquad (B4)$$

the coefficient matrix \bar{A}_{lk} is given by

with

$$a = \frac{l(l+1)}{\omega^2} \frac{4\pi}{3} G \rho_0^* \left[1 - \frac{1}{c^2} \left(\Pi_0 + 4U_0 + \frac{p_0}{\rho_0^*} \right) \right] , \tag{B6}$$

$$c = \frac{3\omega^2}{4\pi G \rho_0^*} \left[1 + \frac{1}{c^2} \left(\Pi_0 + 4U_0 + \frac{p_0}{\rho_0^*} \right) \right] , \tag{B7}$$

$$e = \frac{9}{2\pi G \rho_0^*} \left(U_0 - \Pi_0 - \frac{p_0}{\rho_0} \right) \left(\frac{p_2}{p_0 \Gamma_1} - \frac{\rho_2}{\rho_0} \right) , \tag{B8}$$

$$f = (U_0 - \Pi_0) \frac{3}{\Gamma_1} \frac{\rho_0}{\rho_0} - \frac{3}{\Gamma_1} - 9\left(1 - \frac{3U_0}{c^2}\right) , \tag{B9}$$

and

$$\bar{g} = 3\left[1 + \frac{3}{c^2}(U_0 - \Pi_0)\right] - 3\left[\frac{1}{\Gamma_1} + \frac{3\rho_0}{\rho_0^*} - (U_0 - \Pi_0)\frac{\rho_0}{p_0\Gamma_1}\right]\left[1 + \frac{1}{c^2}\left(\Pi_0 + \frac{p_0}{\rho_0^*}\right)\right] , \tag{B10}$$

Note that, for a realistic matter model we should Taylor expand Γ_1 as well, but here we only consider the simpler case with Γ_1 constant.

Assuming a power law solution $y_i = c_i r^{\lambda}$, we can use computer algebra to solve the matrix problem

$$\det(\bar{A}_{ij} - \lambda \delta_{ij}) = 0 , \qquad (B11)$$

where δ_{ij} is the Kronecker delta, to obtain the set of eigenvalues λ_i and the corresponding eigenvectors Y_i . This way we arrive at the 10 eigenvalues

$$\lambda_{1} = \frac{1}{2} \left(-5 - \sqrt{1 + 4ac} \right) , \ \lambda_{2} = \frac{1}{2} \left(-5 + \sqrt{1 + 4ac} \right) , \ \lambda_{3} = -5 - l , \ \lambda_{4} = -5 - l , \ \lambda_{5} = -5 - l , \ \lambda_{6} = -3 - l , \ \lambda_{7} = -4 + l , \ \lambda_{8} = -4 + l , \ \lambda_{9} = -4 + l , \ \lambda_{10} = -2 + l .$$
 (B12)

Moreover, we have

$$ac = l(l+1) \left[1 - \frac{1}{c^4} \left(\Pi_0 + 4U_0 + \frac{p_0}{\rho_0^*} \right)^2 \right] \approx l(l+1) ,$$
 (B13)

so it follows that

$$\lambda_1 = -3 - l \; , \; \lambda_2 = -2 + l \; .$$
 (B14)

At this point it would seem as if the eigenvalue problem is degenerate—given that we have repeated eigenvalues—so we have to proceed with care. This issue is discussed in [54] but we find their analysis somewhat misleading. The coefficient matrix from (B5) clearly hints at a block-diagonal structure and it is, in fact, straightforward to demonstrate that the equations can be decoupled to show that (even though the eigenvalues are degenerate) the corresponding eigenvectors are linearly dependent.

Discarding the 5 singular solutions (for the physical variables!), we can express the solution to (3.54) as

$$y_i = \sum_{k=1}^5 c_k \mathbf{Y}_k^i r^{\lambda_i} , \qquad (B15)$$

where c_k are constants and Y_k^i represents the *i*-component of the eigenvector associated with the eigenvalue λ_k . Slightly abusing the notation, we relabel the eigenvalues in such a way that $\lambda_2 \to \lambda_1$, $\lambda_7 \to \lambda_2$, $\lambda_8 \to \lambda_3$, $\lambda_9 \to \lambda_4$ and $\lambda_{10} \to \lambda_5$ and identify the associated the associated eigenvectors

$$\boldsymbol{Y}_{1} = \begin{bmatrix} \frac{(3+2l)2a}{(2+l)(ae+fl+f)} \\ \frac{2(3+5l+2l^{2})}{(2+l)(ae+fl+f)} \\ 0 \\ 0 \\ \frac{-3a}{(2+l)(ae+fl+f)} \\ -3a(1+l) \\ 0 \\ 0 \\ 0 \\ \frac{2(3+2l)}{\overline{g}(2+l)} \\ \frac{2}{\overline{g}(2+l)} \\ \frac{1}{2+l} \\ \frac{1}{2} \\$$

Expressing the solution in terms of this basis one can show that the following relations need to be imposed at the centre of the star:

$$y_2 - \frac{1+l}{a}y_1 = 0 , (B17)$$

$$y_4 - ly_3 = 0$$
, (B18)

$$y_6 - (l-1)y_5 + \frac{3y_1 + 2y_3}{3+2l} = 0 , (B19)$$

$$y_8 - ly_7 - \frac{2y_3}{3+2l} = 0 , (B20)$$

$$y_{10} - ly_9 - \frac{ae + fl + f}{a(3+2l)}y_1 - \frac{\bar{g}}{3+2l}y_3 = 0.$$
(B21)

In principle, this completes the argument. However, in order to fully understand the solutions it is worth taking a closer look a how the equations can be decoupled. In order to illustrate the strategy, let us focus on the first of the five solutions.

Consider, first of all, the equations for y_1 and y_2 (obtained from the 2×2 block in the upper left corner of (B5)). The eigenvalues associated with these equations require

$$\begin{vmatrix} \lambda + 3 & -a \\ -c & \lambda + 2 \end{vmatrix} = 0 , \tag{B22}$$

or

$$(\lambda + 3)(\lambda + 2) - ac = 0, (B23)$$

where ac is given by (B13). Discarding the higher order pN terms, we see that the two roots are l-2 and -l-3. The first gives the regular solution at the centre and the corresponding eigenvector is such that

$$y_1 = \frac{a}{l+1}y_2 = \frac{l}{\omega^2} \frac{4\pi G}{3} \rho_0^* \left[1 - \frac{1}{c^2} \left(\Pi_0 + 4U_0 + \frac{p_0}{\rho_0^*} \right) \right] y_2 . \tag{B24}$$

With this relation in hand, we note from (B5) that we need particular integrals for some of the other variables. Clearly, the solution is consistent with $y_3 = y_4 = 0$, but the y_5 and y_6 solutions have to be related in such a way that

$$(l+1)y_5 = y_6 (B25)$$

and

$$[(l+4)(l+1) - l(l+1) + 2] y_5 = 3y_1 = \frac{3a}{l+1}y_2,$$
(B26)

These relations lead to

$$y_5 = \frac{3}{2(2l+3)} \frac{a}{l+1} y_2 \ . \tag{B27}$$

Finally, there is no coupling to y_7 or y_8 , but y_9 and y_{10} are linked by

$$(l+2)y_9 = y_{10} (B28)$$

and

$$[(l+2)(l+3) - l(l+1)] y_9 = 2(2l+3)y_9 = ey_1 + fy_2 = \frac{ae}{l+1}y_2 + fy_2.$$
(B29)

This completes one of the independent solutions to the system. It is, in fact, easy to show that the argument reproduces (up to a constant factor) the Y_2 solution from before.

The step-by-step argument is useful because it allows us to make an additional point. Let us go back to (B23) but this time without neglecting the higher order pN contributions. We then have to solve the quadratic

$$(\lambda + 3) (\lambda + 2) - l(l+1) \left[1 - \frac{1}{c^4} \left(\Pi_0 + 4U_0 + \frac{p_0}{\rho_0^*} \right)^2 \right] = 0.$$
 (B30)

The roots now become

$$\lambda = -\frac{5}{2} \pm \frac{1}{2} \left\{ 1 + 4l(l+1) \left[1 - \frac{1}{c^4} \left(\Pi_0 + 4U_0 + \frac{p_0}{\rho_0^*} \right)^2 \right] \right\}^{1/2} . \tag{B31}$$

This becomes problematic if the argument of the square root changes sign. A necessary condition for this to happen is

$$\frac{1}{c^4} \left(\Pi_0 + 4U_0 + \frac{p_0}{\rho_0^*} \right)^2 > 1 \ . \tag{B32}$$

Ignoring the contributions from the pressure and the internal energy, this corresponds to

$$\frac{4U_0}{c^2} \gtrsim 1 \ . \tag{B33}$$

This clearly never happens in the weak-field regime, but as we demonstrate in the main text the central value of the gravitational potential becomes large enough for this to be an issue when we consider realistic neutron star parameters.

2. At the surface of the star

As mentioned in the main text, at the star's surface we need the Lagrangian perturbation of the pressure to vanish while the potentials δU_l , δX_l and $\delta \psi_l$ and their derivatives are continuous across r = R. Here we provide more details for the boundary conditions for δU_l and δV_l . Starting from (3.23),

$$\frac{1}{r^2}\frac{d}{dr}\left(r^2\frac{d\delta U_l}{dr}\right) - \frac{l(l+1)}{r^2}\delta U_l + 4\pi G\rho^*\left(\frac{\delta p_l}{\Gamma_1 p} - \xi_l^r A + \frac{3\rho}{c^2\rho^*}\delta U_l\right) = 0 \ .$$

Outside the star $\rho^* = 0$, so we have

$$\frac{1}{r^2}\frac{d}{dr}\left(r^2\frac{d\delta U_l}{dr}\right) - \frac{l(l+1)}{r^2}\delta U_l = 0 , \qquad (B34)$$

which leads to

$$\delta U_l = Ar^{-l-1} \tag{B35}$$

where A is a constant. Then δU_l satisfies the condition

$$\frac{d\delta U_l}{dr} + \frac{l+1}{r}\delta U_l = 0 \quad \text{at } r = R ;$$
 (B36)

which leads to

$$y_4 + (l+1)y_3 = 0. (B37)$$

Note that this is the same as in Newtonian case.

Next, for the vector potential δV_l^r , the equation with ρ^* vanishing outside the star, turns into

$$\frac{1}{r^2}\frac{d}{dr}\left(r^2\frac{d\delta V_l^r}{dr}\right) + \frac{2}{r}\frac{d\delta V_l^r}{dr} + \frac{2-l(l+1)}{r^2}\delta V_l^r = -\frac{2}{r}\delta U_l , \qquad (B38)$$

i.e., a non-homogeneous linear differential equation. The general solution should be the sum of the particular solution and the solution to the corresponding complementary equation. As δU_l behaves like r^{-l-1} , we can then tell from (B38) that the particular solution should have the form

$$\delta V_{l p}^r = B_1 r^{-l} . ag{B39}$$

We can get a relation between the constant A and B_1 by substituting the particular solution back into the equation:

$$B_1(2l-1) = A {.} {(B40)}$$

Assuming the solution to complementary equation of (B38)

substituting into the complementary equation

$$\beta(\beta+1)r^{\beta} + 2\beta r^{\beta} + [2-l(l+1)r^{\beta}] = 0$$

we find that

$$\beta = l + 1, -l - 2 \tag{B42}$$

where $\beta = -l - 2$ ensures that δV_l^r is regular at infinity for $l \geq 2$. Therefore the solution to (B38) should take the form

$$\delta V_l^r = B_1 r^{-l} + B_2 r^{-l-2} = \frac{A}{(2l-1)r^l} + \frac{B_2}{r^{l+2}},$$
(B43)

while its derivative is

$$\frac{d\delta V_l^r}{dr} = -B_1 l r^{-l-1} - (l+2)B_2 r^{-l-3} = -\frac{Al}{(2l-1)r^{l+1}} - \frac{B_2(l+2)}{r^{l+3}}.$$
 (B44)

Eliminating the constant B_2 from (B43)(B44), we arrive at

$$(l+2)y_5 + y_6 = \frac{2y_3}{2l-1} \,. \tag{B45}$$

Similarly, we can work out the conditions for the potentials δX_l and $\delta \psi_l$.

Appendix C: Keeping higher order terms

Having identified the issue associated with the Taylor expansion at the centre of the star, we want to see if there is an "easy" fix to the numerical problem. One possible strategy proceeds as as follows: In the steps going from (3.21) to (3.40), we multiplied by

$$\frac{1}{\rho g} \left(1 - \frac{2U}{c^2} \right)$$

expanded the result and kept only the 1pN terms. For example, we had

$$\left(1 - \frac{2U}{c^2}\right) \times \left(1 + \frac{2U}{c^2}\right) A \frac{dp}{dr} r y_1 = \left(1 - \frac{4U^2}{c^4}\right) A \frac{dp}{dr} r y_1 \approx A \frac{dp}{dr} r y_1.$$

This last step is evidently not valid in the neutron star regime. A simple alternative is to, rather than expanding, simply divide by the term including the gravitational potential. Then, in place of (3.40) we have for y_2 :

$$\begin{split} r\frac{dy_2}{dr} &= c_1\tilde{\omega}^2 \left[1 + \frac{1}{c^2} \left(\Pi + 3U + \frac{p}{\rho^*} \right) \right] \frac{\rho^*}{\rho} \left(1 + \frac{2U}{c^2} \right)^{-1} y_1 + \frac{A^*}{\rho g} \frac{dp}{dr} y_1 \\ &\quad + \left(A^* - \frac{r}{g} \frac{dg}{dr} - 1 \right) y_2 + \frac{1}{\rho^* c^2} \frac{dp}{dr} \left(1 + \frac{2U}{c^2} \right)^{-1} r y_2 \\ &\quad + A^* \left[1 + \frac{1}{c^2} \left(\Pi + \frac{p}{\rho^*} \right) \right] y_3 - \frac{1}{c^2} \left(\frac{d\Pi}{dr} + \frac{1}{\rho^*} \frac{dp}{dr} - \frac{p}{\rho^*} \frac{d\rho^*}{dr} \right) r y_3 \\ &\quad + \frac{1}{\rho^* c^2} \frac{dp}{dr} \left(1 + \frac{2U}{c^2} \right)^{-1} r \left[1 + \frac{1}{c^2} \left(\Pi + \frac{p}{\rho^*} \right) \right] y_3 + \frac{4}{\rho c^2} \left(\frac{dp}{dr} - \rho^* \frac{dU}{dr} \right) \left(1 + \frac{2U}{c^2} \right)^{-1} r y_3 \\ &\quad + \frac{\rho^*}{\rho} \left[1 + \frac{1}{c^2} \left(\Pi - U + \frac{p}{\rho^*} \right) \right] \left(1 + \frac{2U}{c^2} \right)^{-1} y_4 - \left[1 + \frac{1}{c^2} \left(\Pi + \frac{p}{\rho^*} \right) \right] y_4 \\ &\quad - \frac{\rho^*}{\rho} \left(1 + \frac{2U}{c^2} \right)^{-1} \left(c_1 \tilde{\omega}^2 \frac{4gr}{c^2} y_5 - c_1 \tilde{\omega}^2 \frac{gr}{2c^2} y_8 - \frac{1}{c^2} gr y_{10} \right) \; . \end{split}$$
 (C1)

Similarly for y_1 , instead of (3.39), we have:

$$r\frac{dy_{1}}{dr} = -\left(A^{*} + \frac{r}{\rho^{*}}\frac{d\rho^{*}}{dr} + 3\right)y_{1} - V_{g}y_{2} + \frac{\rho}{\rho^{*}}\left(1 + \frac{2U}{c^{2}}\right)\left[1 + \frac{1}{c^{2}}\left(\Pi + 3U + \frac{p}{\rho^{*}}\right)\right]^{-1}\frac{l(l+1)}{c_{1}\tilde{\omega}^{2}}y_{2}$$

$$-V_{g}\left[1 + \frac{1}{c^{2}}\left(\Pi + \frac{p}{\rho^{*}}\right)\right]y_{3} + \frac{\rho}{\rho^{*}}\left(1 + \frac{2U}{c^{2}}\right)\left[1 + \frac{1}{c^{2}}\left(\Pi + \frac{p}{\rho^{*}}\right)\right]\left[1 + \frac{1}{c^{2}}\left(\Pi + 3U + \frac{p}{\rho^{*}}\right)\right]^{-1}\frac{l(l+1)}{c_{1}\tilde{\omega}^{2}}y_{3}$$

$$+ \frac{gr}{c^{2}}\left[1 + \frac{1}{c^{2}}\left(\Pi + 3U + \frac{p}{\rho^{*}}\right)\right]^{-1}y_{3} - \left[1 + \frac{1}{c^{2}}\left(\Pi - U + \frac{p}{\rho^{*}}\right)\right]\left[1 + \frac{1}{c^{2}}\left(\Pi + 3U + \frac{p}{\rho^{*}}\right)\right]^{-1}\frac{l(l+1)}{c_{1}\tilde{\omega}^{2}}y_{3}$$

$$+ \left[1 + \frac{1}{c^{2}}\left(\Pi + 3U + \frac{p}{\rho^{*}}\right)\right]^{-1}\left[\frac{4gr}{c^{2}}(2y_{5} + y_{6}) - \frac{gr}{2c^{2}}l(l+1)y_{7} - \frac{grl(l+1)}{c^{2}}y_{9}\right].\right] (C2)$$

Using these two equations in place of the original ones we find that the numerical problems at the centre of the star can be avoided. This strategy is pragmatic and may seem somewhat ad hoc, but it serves as a demonstration of how the problems we encounter with the pN mode calculation can be circumvented.

- [1] R. Kumar, V. Dexheimer, J. Jahan, J. Noronha, J. Noronha-Hostler, C. Ratti, N. Yunes, A. R. Nava Acuna, M. Alford, M. H. Anik, D. Chatterjee, K. Chatziioannou, H.-Y. Chen, A. Clevinger, C. Conde, N. Cruz-Camacho, T. Dore, C. Drischler, H. Elfner, R. Essick, D. Friedenberg, S. Ghosh, J. Grefa, R. Haas, A. Haber, J. Hammelmann, S. Harris, C.-J. Haster, T. Hatsuda, M. Hippert, R. Hirayama, J. W. Holt, M. Kahangirwe, J. Karthein, T. Kojo, P. Landry, Z. Lin, M. Luzum, T. A. Manning, J. Salinas San Martin, C. Miller, E. R. Most, D. Mroczek, A. Muronga, N. Patino, J. Peterson, C. Plumberg, D. Price, C. Providencia, R. Rougemont, S. Roy, H. Shah, S. Shapiro, A. W. Steiner, M. Strickland, H. Tan, H. Togashi, I. Portillo Vazquez, P. Wen, Z. Zhang, and Muses Collaboration, Theoretical and experimental constraints for the equation of state of dense and hot matter, Living Reviews in Relativity 27, 3 (2024).
- [2] M. C. Miller, F. K. Lamb, A. J. Dittmann, S. Bogdanov, Z. Arzoumanian, K. C. Gendreau, S. Guillot, A. K. Harding, W. C. G. Ho, J. M. Lattimer, R. M. Ludlam, S. Mahmoodifar, S. M. Morsink, P. S. Ray, T. E. Strohmayer, K. S. Wood, T. Enoto, R. Foster, T. Okajima, G. Prigozhin, and Y. Soong, Psr j0030+0451 mass and radius from nicer data and implications for the properties of neutron star matter, The Astrophysical Journal Letters 887, L24 (2019).
- [3] T. E. Riley, A. L. Watts, S. Bogdanov, P. S. Ray, R. M. Ludlam, S. Guillot, Z. Arzoumanian, C. L. Baker, A. V. Bilous, D. Chakrabarty, K. C. Gendreau, A. K. Harding, W. C. G. Ho, J. M. Lattimer, S. M. Morsink, and T. E. Strohmayer, A nicer view of psr j0030+0451: Millisecond pulsar parameter estimation, The Astrophysical Journal Letters 887, L21 (2019).
- [4] T. Salmi, D. Choudhury, Y. Kini, T. E. Riley, S. Vinciguerra, A. L. Watts, M. T. Wolff, Z. Arzoumanian, S. Bogdanov, D. Chakrabarty, K. Gendreau, S. Guillot, W. C. G. Ho, D. Huppenkothen, R. M. Ludlam, S. M. Morsink, and P. S. Ray, The radius of the high-mass pulsar psr j0740+6620 with 3.6 yr of nicer data, The Astrophysical Journal 974, 294 (2024).
- [5] A. J. Dittmann, M. C. Miller, F. K. Lamb, I. M. Holt, C. Chirenti, M. T. Wolff, S. Bogdanov, S. Guillot, W. C. G. Ho, S. M. Morsink, Z. Arzoumanian, and K. C. Gendreau, A more precise measurement of the radius of psr j0740+6620 using updated nicer data, The Astrophysical Journal 974, 295 (2024).
- [6] E. E. Flanagan and T. Hinderer, Constraining neutron-star tidal love numbers with gravitational-wave detectors, Phys. Rev. D 77, 021502 (2008).
- [7] K. Chatziioannou, Neutron-star tidal deformability and equation-of-state constraints, General Relativity and Gravitation 52, 109 (2020).
- [8] B. P. Abbott et al. (LIGO Scientific Collaboration and Virgo Collaboration), Gw170817: Observation of gravitational waves from a binary neutron star inspiral, Phys. Rev. Lett. 119, 161101 (2017).
- [9] B. P. Abbott *et al.* (The LIGO Scientific Collaboration and the Virgo Collaboration), Gw170817: Measurements of neutron star radii and equation of state, Phys. Rev. Lett. **121**, 161101 (2018).
- [10] B. P. Abbott *et al.*, Gw190425: Observation of a compact binary coalescence with total mass $\sim 3.4 \text{ m}_{\odot}$, The Astrophysical Journal Letters 892, L3 (2020).
- [11] M. Maggiore, C. V. D. Broeck, N. Bartolo, E. Belgacem, D. Bertacca, M. A. Bizouard, M. Branchesi, S. Clesse, S. Foffa, J. García-Bellido, S. Grimm, J. Harms, T. Hinderer, S. Matarrese, C. Palomba, M. Peloso, A. Ricciardone, and M. Sakellariadou, Science case for the einstein telescope, Journal of Cosmology and Astroparticle Physics 2020 (03), 050.
- [12] D. Reitze *et al.*, Cosmic Explorer: The U.S. Contribution to Gravitational-Wave Astronomy beyond LIGO, arXiv:1907.04833 [astro-ph.IM] (2019).
- [13] K. Chatziioannou, Uncertainty limits on neutron star radius measurements with gravitational waves, Phys. Rev. D 105, 084021 (2022).
- [14] T. Hinderer, A. Taracchini, F. Foucart, A. Buonanno, J. Steinhoff, M. Duez, L. E. Kidder, H. P. Pfeiffer, M. A. Scheel, B. Szilagyi, K. Hotokezaka, K. Kyutoku, M. Shibata, and C. W. Carpenter, Effects of Neutron-Star Dynamic Tides on Gravitational Waveforms within the Effective-One-Body Approach, Phys. Rev. Lett. 116, 181101 (2016).

- [15] J. Steinhoff, T. Hinderer, A. Buonanno, and A. Taracchini, Dynamical tides in general relativity: Effective action and effective-one-body Hamiltonian, Phys. Rev. D 94, 104028 (2016).
- [16] N. Andersson and P. Pnigouras, Exploring the effective tidal deformability of neutron stars, Phys. Rev. D 101, 083001 (2020).
- [17] G. Pratten, P. Schmidt, and T. Hinderer, Gravitational-wave asteroseismology with fundamental modes from compact binary inspirals, Nature Communications 11, 2553 (2020).
- [18] D. Lai, Resonant oscillations and tidal heating in coalescing binary neutron stars, Monthly Notices of the Royal Astronomical Society 270, 611 (1994).
- [19] K. D. Kokkotas and G. Schaefer, Tidal and tidal-resonant effects in coalescing binaries, Monthly Notices of the Royal Astronomical Society 275, 301 (1995).
- [20] W. C. G. Ho and N. Andersson, New dynamical tide constraints from current and future gravitational wave detections of inspiralling neutron stars, Phys. Rev. D 108, 043003 (2023).
- [21] D. Tsang, J. S. Read, T. Hinderer, A. L. Piro, and R. Bondarescu, Resonant Shattering of Neutron Star Crusts, Phys. Rev. Lett. 108, 011102 (2012).
- [22] Z. Pan, Z. Lyu, B. Bonga, N. Ortiz, and H. Yang, Probing Crust Meltdown in Inspiraling Binary Neutron Stars, Phys. Rev. Lett. 125, 201102 (2020).
- [23] J. Zhu, C. Wang, C. Xia, E. Zhou, and Y. Ma, Probing phase transitions in neutron stars via the crust-core interfacial mode, Phys. Rev. D 107, 083023 (2023).
- [24] Z. Miao, E. Zhou, and A. Li, Resolving Phase Transition Properties of Dense Matter through Tidal-excited g-mode from Inspiralling Neutron Stars, Astrophys. J. 964, 31 (2024).
- [25] A. Counsell, F. Gittins, N. Andersson, and I. Tews, Interface modes in inspiralling neutron stars: A gravitational-wave probe of first-order phase transitions, preprint arXiv:2504.06181 (2025).
- [26] J. Steinhoff, T. Hinderer, T. Dietrich, and F. Foucart, Spin effects on neutron star fundamental-mode dynamical tides: Phenomenology and comparison to numerical simulations, Physical Review Research 3, 033129 (2021).
- [27] P. Pnigouras, F. Gittins, A. Nanda, N. Andersson, and D. I. Jones, The dynamical tides of spinning Newtonian stars, Monthly Notices of the Royal Astronomical Society 527, 8409 (2024).
- [28] H. Yu, P. Arras, and N. N. Weinberg, Dynamical tides during the inspiral of rapidly spinning neutron stars: Solutions beyond mode resonance, Phys. Rev. D 110, 024039 (2024).
- [29] K. H. Lockitch, N. Andersson, and J. L. Friedman, Rotational modes of relativistic stars: Analytic results, Phys. Rev. D 63, 024019 (2000).
- [30] N. Andersson and F. Gittins, Formulating the r-mode problem for slowly rotating neutron stars, The Astrophysical Journal 945, 139 (2023).
- [31] É. É. Flanagan and É. Racine, Gravitomagnetic resonant excitation of Rossby modes in coalescing neutron star binaries, Phys. Rev. D 75, 044001 (2007).
- [32] E. Poisson, Gravitomagnetic tidal resonance in neutron-star binary inspirals, Phys. Rev. D 101, 104028 (2020).
- [33] J. L. Friedman and B. F. Schutz, Lagrangian perturbation theory of nonrelativistic fluids., Astrophys. J. 221, 937 (1978).
- [34] A. K. Schenk, P. Arras, É. É. Flanagan, S. A. Teukolsky, and I. Wasserman, Nonlinear mode coupling in rotating stars and the r-mode instability in neutron stars, Phys. Rev. D 65, 024001 (2001).
- [35] K. S. Thorne and A. Campolattaro, Non-Radial Pulsation of General-Relativistic Stellar Models. I. Analytic Analysis for $l \geq 2$, Astrophysical Journal, vol. 149, p.591 (1967).
- [36] R. Price and K. S. Thorne, Non-Radial Pulsation of General-Relativistic Stellar Models. II. Properties of the Gravitational Waves, Astrophys. J. 155, 163 (1969).
- [37] K. S. Thorne, Nonradial Pulsation of General-Relativistic Stellar Models. III. Analytic and Numerical Results for Neutron Stars, Astrophys. J. 158, 1 (1969).
- [38] K. S. Thorne, Nonradial Pulsation of General-Relativistic Stellar Models.IV. The Weakfield Limit, Astrophys. J. 158, 997 (1969).
- [39] L. Lindblom and S. L. Detweiler, The quadrupole oscillations of neutron stars., Astrophysical Journal Supplement Series 53, 73 (1983).
- [40] S. Detweiler and L. Lindblom, On the nonradial pulsations of general relativistic stellar models, Astrophys. J. 292, 12 (1985).
- [41] N. Andersson, A gravitational-wave perspective on neutron-star seismology, Universe 7, 10.3390/universe 7040097 (2021).
- [42] T. Pitre and E. Poisson, General relativistic dynamical tides in binary inspirals without modes, Phys. Rev. D 109, 064004 (2024).
- [43] A. Hegade K. R., J. L. Ripley, and N. Yunes, Dynamical tidal response of nonrotating relativistic stars, Phys. Rev. D 109, 104064 (2024).
- [44] R. Abhishek Hegade K., K. J. Kwon, T. Venumadhav, H. Yu, and N. Yunes, Relativistic and Dynamical Love, arXiv e-prints, arXiv:2507.10693 (2025).
- [45] Z. Miao, X. Feng, Z. Pan, and H. Yang, Relativistic excitation of compact stars, arXiv e-prints, arXiv:2506.23176 (2025).
- [46] N. Andersson, F. Gittins, S. Yin, and R. P. Macedo, Building post-newtonian neutron stars, Classical and Quantum Gravity 40, 025016 (2023).
- [47] F. Gittins, N. Andersson, and S. Yin, Perturbation theory for post-Newtonian neutron stars, Classical and Quantum Gravity 42, 135014 (2025).
- [48] E. Poisson and C. M. Will, Gravity (Cambridge University Press, 2014).

- [49] C. Cutler and L. Lindblom, Post-Newtonian effects on the oscillations of rotating stars., Annals of the New York Academy of Sciences 631, 97 (1991).
- [50] S. R. Boston, C. R. Evans, and J. C. Clemens, Relativistic corrections in white dwarf asteroseismology, The Astrophysical Journal 952, 87 (2023).
- [51] A. F. Fantina, N. Chamel, J. M. Pearson, and S. Goriely, Neutron star properties with unified equations of state of dense matter*, Astronmy & Astrophysics 559, 10.1051/0004-6361/201321884 (2013).
- [52] S. Goriely, N. Chamel, and J. M. Pearson, Further explorations of Skyrme-Hartree-Fock-Bogoliubov mass formulas. XIII. The 2012 atomic mass evaluation and the symmetry coefficient, Phys. Rev. C 88, 024308 (2013).
- [53] S. Chandrasekhar, The Stability of Gaseous Masses for Radial and Non-Radial Oscillations in the Post-Newtonian Approximation of General Relativity., Astrophys. J. 142, 1519 (1965).
- [54] W. Unno, Y. Osaki, H. Ando, and H. Shibahashi, Nonradial oscillations of stars (University of Tokyo Press, 1979).
- [55] A. R. Counsell, F. Gittins, and N. Andersson, The impact of nuclear reactions on the neutron-star g-mode spectrum, Monthly Notices of the Royal Astronomical Society **531**, 1721 (2024).
- [56] W. A. Dziembowski, Nonradial Oscillations of Evolved Stars. I. Quasiadiabatic Approximation, Acta Astronomica 21, 289 (1971).
- [57] K. D. Kokkotas and B. F. Schutz, W-modes: a new family of normal modes of pulsating relativistic stars, Monthly Notices of the Royal Astronomical Society 255, 119 (1992).
- [58] C. J. Krüger, W. C. G. Ho, and N. Andersson, Seismology of adolescent neutron stars: Accounting for thermal effects and crust elasticity, Phys. Rev. D 92, 063009 (2015).
- [59] M. Shibata, Numerical study of synchronized binary neutron stars in the post-newtonian approximation of general relativity, Phys. Rev. D 55, 6019 (1997).
- [60] A. R. Counsell, F. Gittins, and N. Andersson, The impact of nuclear reactions on the neutron-star g-mode spectrum, Monthly Notices of the Royal Astronomical Society 531, 1721 (2024).
- [61] S. Yin, Data for "a post-newtonian approach to neutron star oscillations" (2025), https://doi.org/10.5281/zenodo. 16814062.
- [62] N. Andersson and P. Pnigouras, The g-mode spectrum of reactive neutron star cores, Monthly Notices of the Royal Astronomical Society 489, 4043 (2019).